In-situ Transmission Electron Microscopy

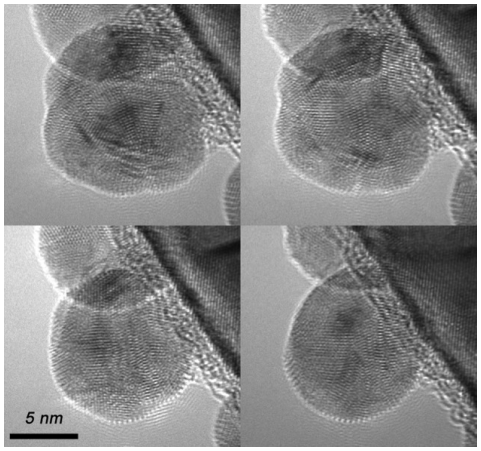

1

"In-Situ" Microscopy & Microanalysis

Observation of the State of a material during Dynamic conditions

- **Dynamic Conditions**
  - Temporal
  - Temperature
  - Stress/Strain/Mechanical Deformation
  - Vacuum/Gaseous/Liquid Environment
  - EM Fields
  - Irradiation Environment
    - Charged Particles
    - Photons
- **State**
  - Morphology
  - Crystallography
  - Bonding/Electronic Structure
  - Elemental/Chemical Constituents

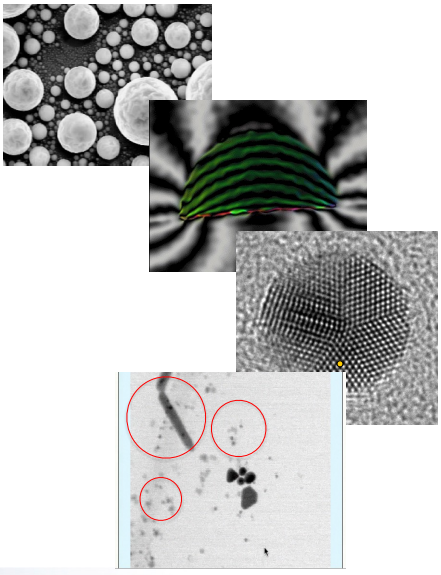

2

What is "In-Situ" Microscopy/Microanalysis

Observation of the State of a material during Dynamic conditions

- *State*
  - *Morphology*
  - *Crystallography*
  - *Elemental/Chemical Constituents*
  - *Bonding/Electronic State*
- *Dynamic Conditions*
  - *Temporal*
  - *Temperature*
  - *Stress/Strain/Mechanical Deformation*
  - *Vacuum/Gaseous/Liquid Environment*
  - *EM Fields*
  - *Irradiation Environment*
    - *Charged Particles*
    - *Photons*

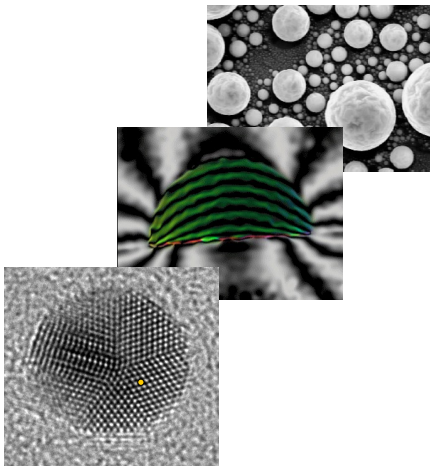

3

Ex-Situ TEM Post-Mortem Experiments

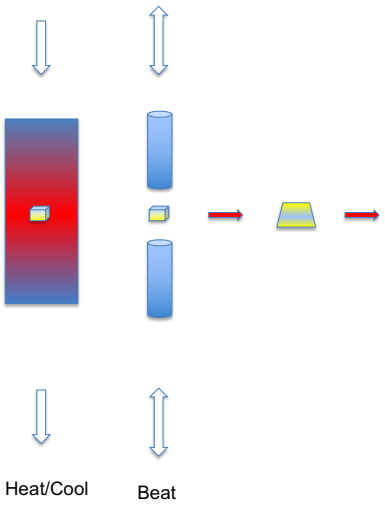

4

ANL has a Long History in In-situ Experimentation in the EM

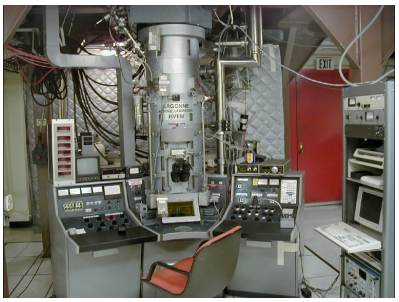

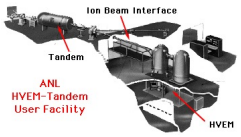

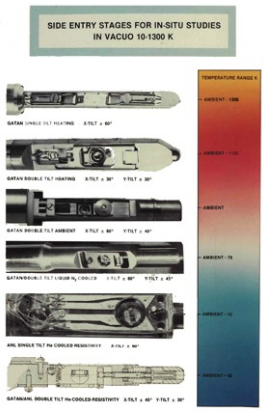

Decommissioned Fall 2001

5

In-situ Characterization: The game is changing

- *Improved Electron Optics*
  - *Improved Performance*
  - *Potentially Improved Experimental Space*
  - *In-Situ Holders/Environments*
- *Improved Detector/Geometry*
  - *Higher Resolution*
  - *Higher Speed DAQ*
  - *Higher Efficiency*
- *Computationally Mediated Experiments*
  - *Exploit Electron Solid Interactions for State-of-the-Art Materials Characterization*

New Challenges:

- *In-situ observation of growth processes - at atomic resolution in growth environment*
- *Simultaneous imaging of hard/soft components*
- *Dynamics - Fast detection schemes, detectors, and sources*
- *In-situ / high-spatial resolution elemental spectroscopy*

6

"In-Situ Holders" Today
Cover a wide range of Conditions

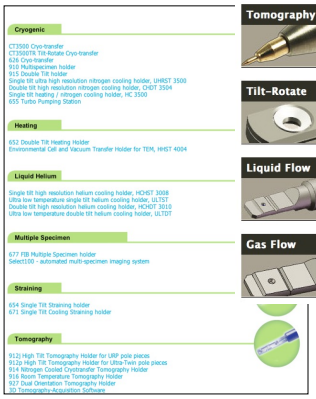

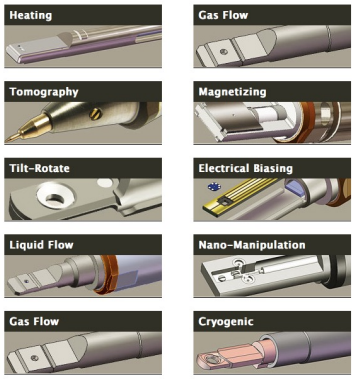

7

Piezo Controled Mechanical Probe & TEM/STEM

[1] D. B. Bogy, *J. Appl. Mech.*, **35** (1968) 460-466.

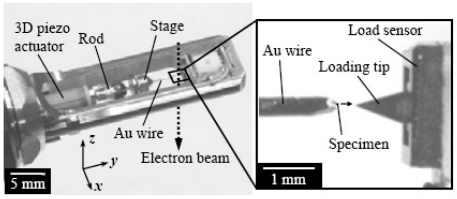

FIG. 1. Mechanical loading apparatus built into specimen holder.

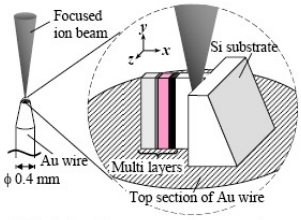

FIG. 2. Specimen preparation procedure.

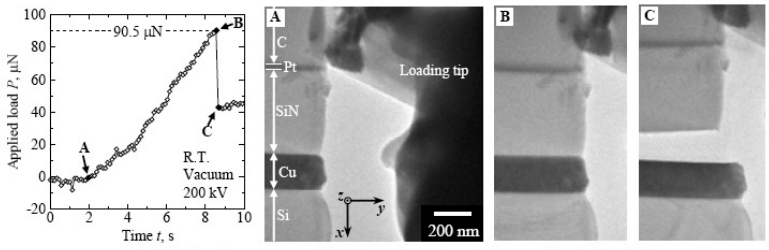

FIG. 3. Loading curve and TEM snapshots of specimen at points A, B and C.

8

In-situ Deformation

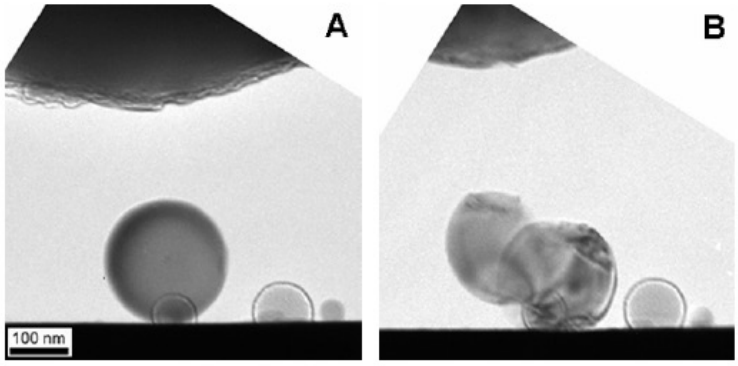

Dynamic Studies in the TEM: *In-Situ* Compression of Nanoparticles

Julia Deneen[1], William W. Mook[1], Andrew M. Minor[2], William W. Gerberich, and C. Barry Carter[1*]

[1] Department of Chemical Engineering and Materials Science, University of Minnesota, 421 Washington Ave SE, Minneapolis, MN 55455, USA.
[2] Ernest Orlando Lawrence Berkeley National Laboratory, National Center For Electron Microscopy, One Cyclotron Rd, MS 72-150, Berkeley, CA 94720, USA.
Correspondence: deneen@cems.umn.edu

9

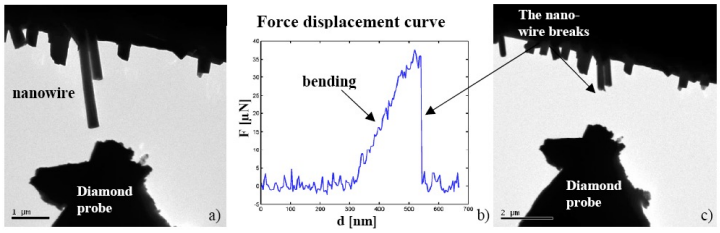

Fig. 1: In situ nanowire measurement (a) The sample is moved towards the diamond probe which is mounted on thc force sensor. (b) Obtained force as a function of the distance moved towards the diamond probe (c) The nanowire after measurement.

In situ TEM-nanoindentation using a MEMS Force Sensor

A. Nafari[1,2*], M.W. Larsson[2,3], A. Danilov[2], H.Olin[4], K. Svensson[1], P. Enoksson[1]

[1]Chalmers University of Technology, SE-41296 Gothenburg, SWEDEN;
[2]Nanofactory Instruments AB, Wallerisgatan 2, SE-41258 Gothenburg, SWEDEN;
[3]Lund University, SE-22100 Lund, SWEDEN;
[4]Mid Sweden University, SE-85170 Sundsvall, SWEDEN;
Correspondence: alexandra.nafari@nanofactory.com

10

Gas Injection System

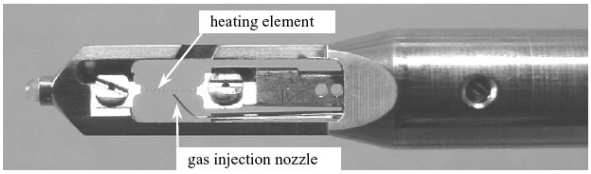

Fig.1 A gas injection-specimen heating holder developed for use with conventional TEMs.

Environmental transmission electron microscopy using a conventional TEM and a gas injection-specimen heating holder

T. Kamino*, T.Yaguchi*, A.Watabe*, H.Saka** and K.Kishita***
* Hitachi High-Technologies Corp., 11-1 Ishikawa-cho, Hitachinaka, Ibaraki, 312-0057 Japan
**Nagoya University, Furo-cho, Chikusa-ku, Nagoya, 4642-8603 Japan
*** Material Analysis Dept. Toyota Motors Corp., 1 Toyota-cho, Toyota 471-8572 Japan

11

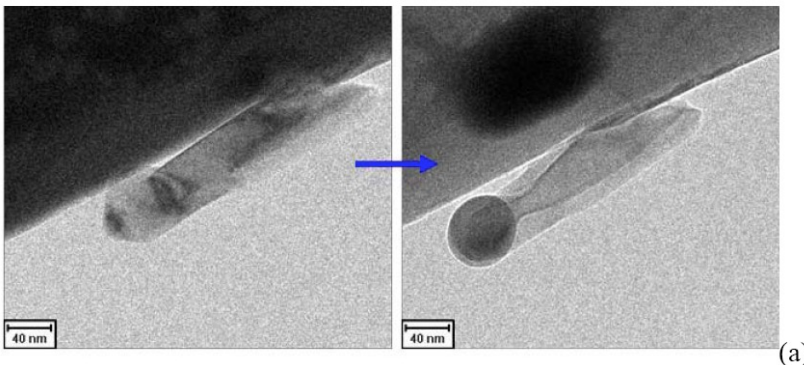

M.L. Taheri,* B.S. Simpkins, ** T. Lagrange,* B.W. Reed*, N. Teslich,* and N.D. Browning *

* Chemistry, Materials & Life Sciences Division, Lawrence Livermore National Laboratory, PO Box 808, Livermore, CA 94550
** Chemistry Division, Naval Research Laboratory, Washington, DC 20375

12

Original In-situ Furnace Heater Geometry

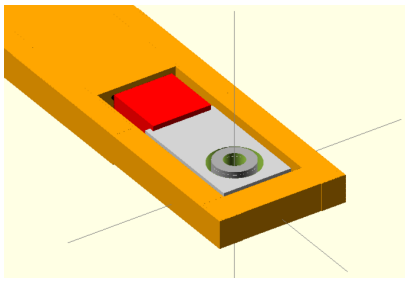

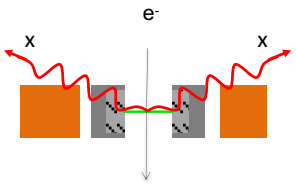

Significant Challenges
due to the furnace design

13

Membrane Heater Geometry

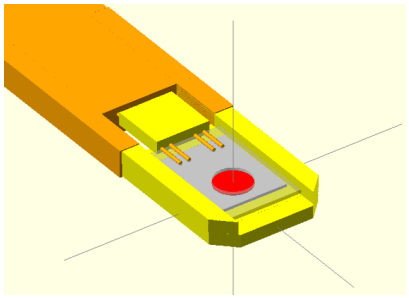

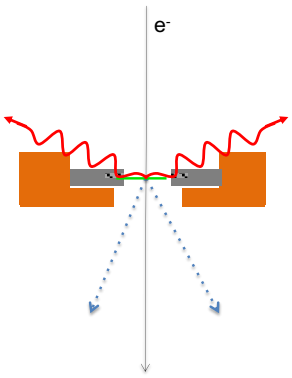

14

Membrane Heater Geometry

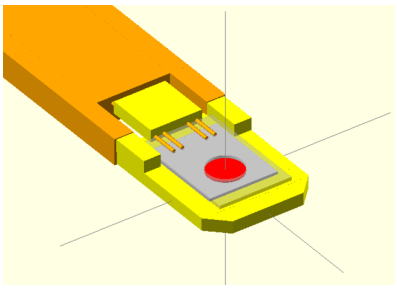

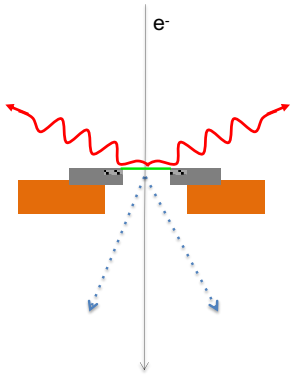

15

SiC/SiN RT vs 400 C

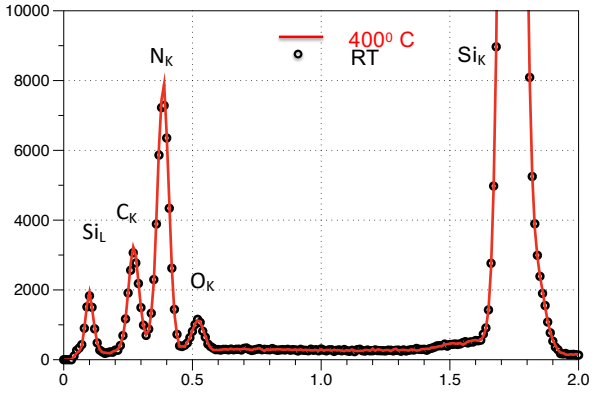

Windowless SDD

16

Spectral Distortions in *Windowless SDD's* are due to
Infra-Red Emission Signal at Low Energies swamping amplifiers
Loss of Resolution and Spectral Shifts

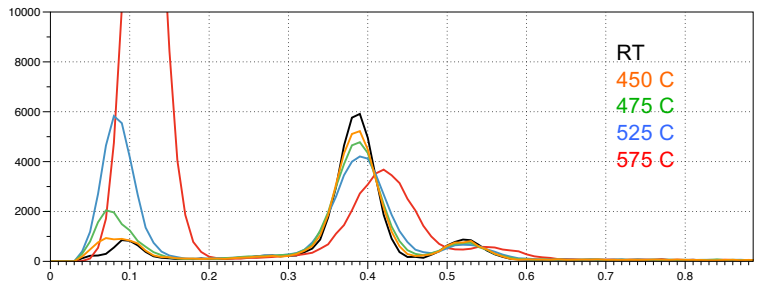

Spectral Response = f(Z, Temp, Detector Geometry & Electronics)

17

Amplifier Time Constant reset from 3.8 µsec to 120 ns
Windowless SDD's to extend Temperature Range to mitigate Infra-Red Emission

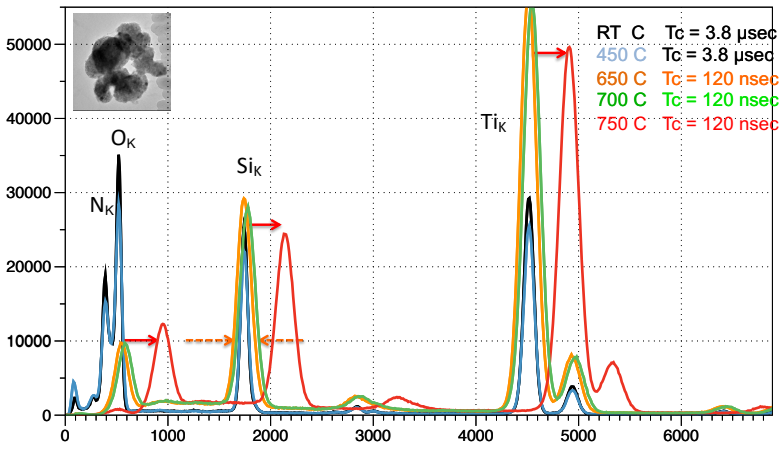

Peaks broaden and shift to higher energies with IR signal swamping electronics
Detector Time Constant extends range to 700 C+

18

XEDS Modified Holder– 50 nm SiN Window in Vacuum

Sintered Pd on TiO_2 Segregation after in-situ Heating to 500^{o} C

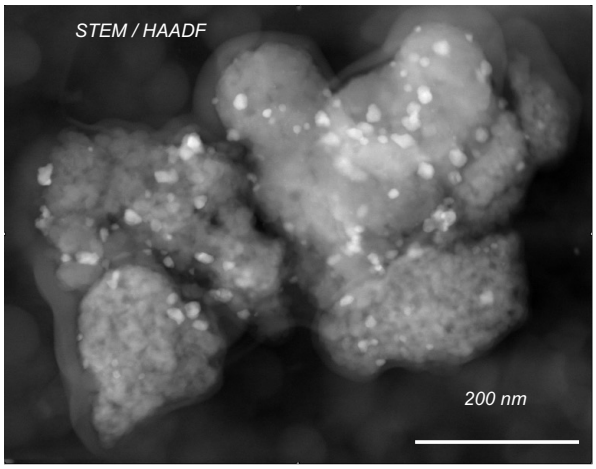

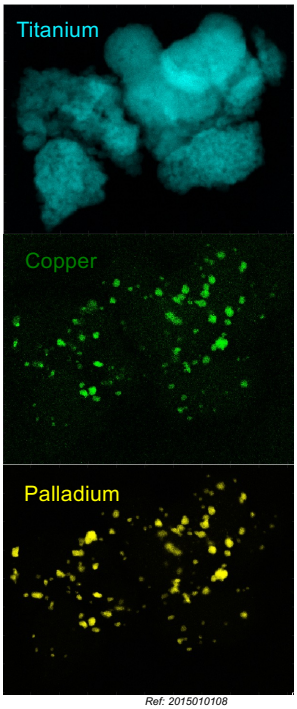

Ref: 2015010108

19

XEDS Modified Holder– 50 nm SiN Window in Vacuum @ 100° C

NP Surface Segregation/Sintering on $CaTiO_3$

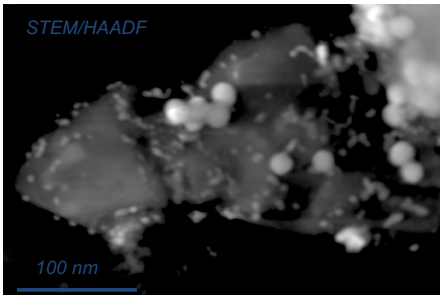

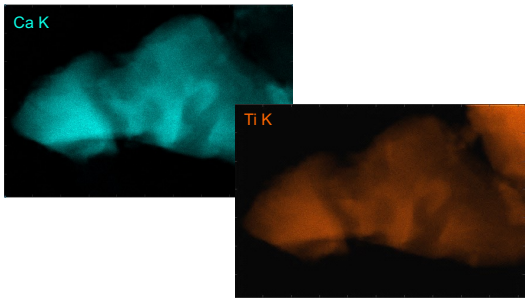

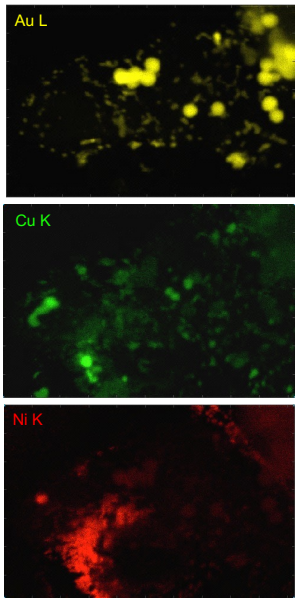

Ref: 2015011715

20

"Conventional" EM

Dry - Conductive Specimens

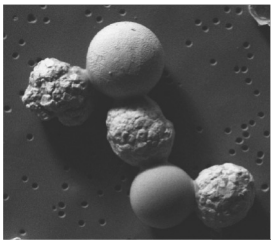

"Environmental" EM

Biological
Non-Conductive
Gaseous/Moist/Liquid

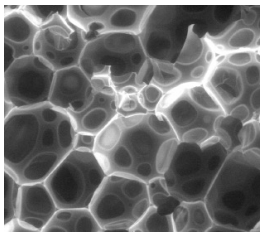

21

Environmental Microscopy

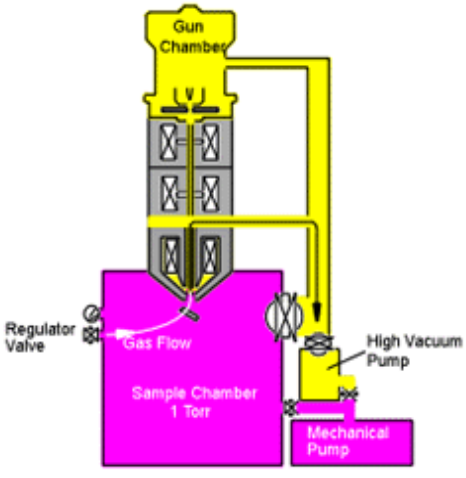

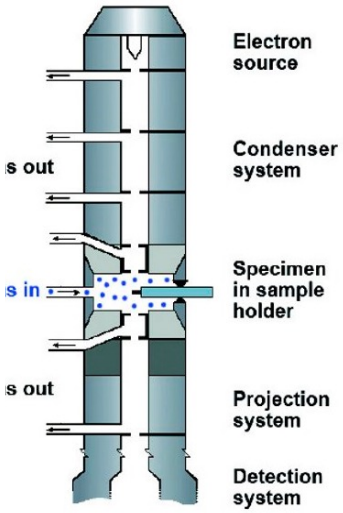

ESEM vs ETEM

22

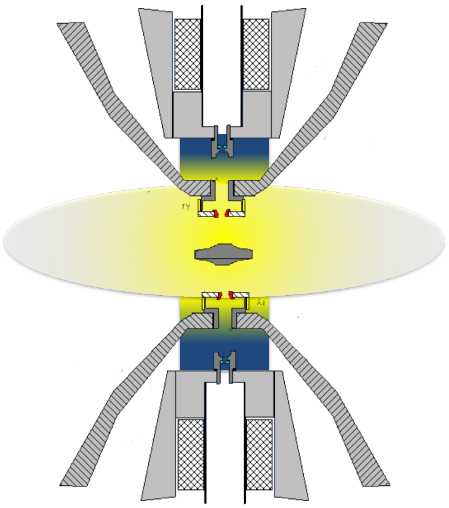

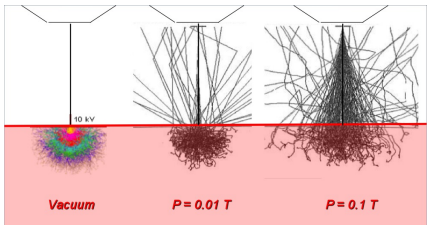

Beam Gas Path

23

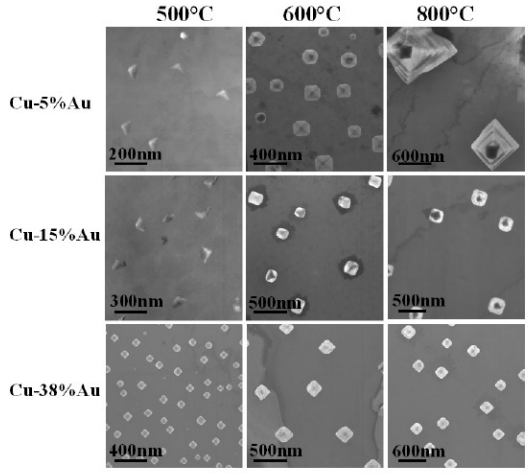

The Surface Kinetics of Cu and Cu Alloy Nano-oxidation

Judith C. Yang[1*], Li Sun[1], Xuetian Han[1], Guangwen Zhou[2] and Jeffrey E. Eastman[2]

[1]University of Pittsburgh, 848 Benedum Hall, Pittsburgh, PA, 15261, USA
[2]Argonne National Laboratory, 9700 S. Cass Ave, Argonne, IL, 60439, USA
Correspondence: jyang@engr.pitt.edu

24

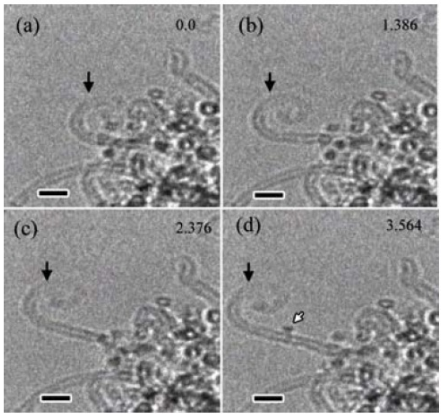

In-Situ TEM Studies of Carbon Nanotube Growth By Catalytic Decomposition of Acetylene

R. Sharma[1*], G.H. Du[1], P. Rez[2] and M. M. J. Treacy[2]

[1]Center for Solid State Science, Arizona State University, Tempe, AZ 85287
[2]Dept. of Physics and Astronomy, Arizona State University, Tempe, AZ 85287
Correspondence: Renu.Sharma@asu.edu

25

Environmental TEM Systems

Differential Pumping (ETEM) vs In-situ eCells

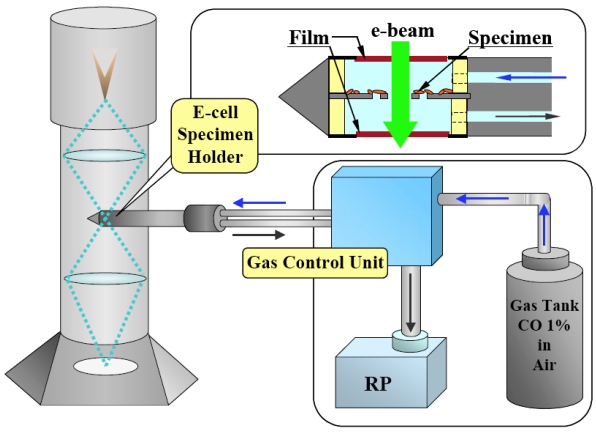

26

In-Situ Cells

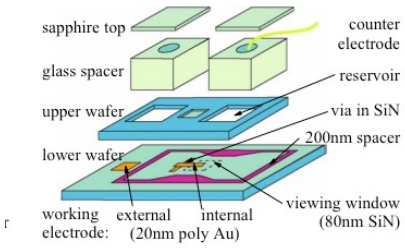

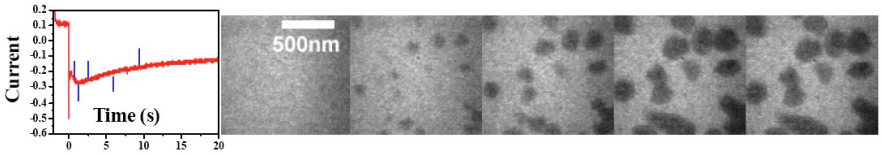

***In situ* Microscopy of Electrochemical Reactions**

F. M. Ross, A. Radisic[*,+], P. Vereecken[+], J. B. Hannon, and P. C. Searson[*]

IBM T. J. Watson Research Center
1101 Kitchawan Road, Yorktown Heights, New York 10598, USA
[*]Department of Materials Science and Engineering
Johns Hopkins University, Baltimore, Maryland 21218, USA
[+]Present address: Interuniversity MicroElectronics Center, B-3001 Leuven, Belgium
Correspondence: fmross@us.ibm.com

27

Penumbra of the specimen holder
Is a limiting factor for XEDS in virtually all experiments
particularly during in-situ configurations

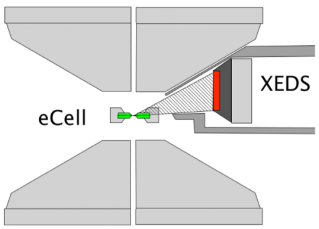

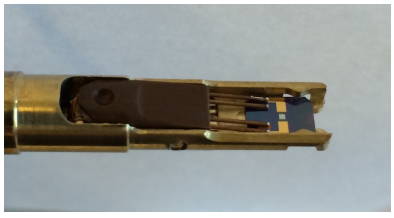

28

Holder Penumbra in Gaseous and Liquid eCell Holders

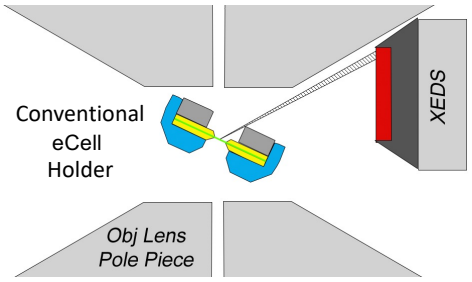

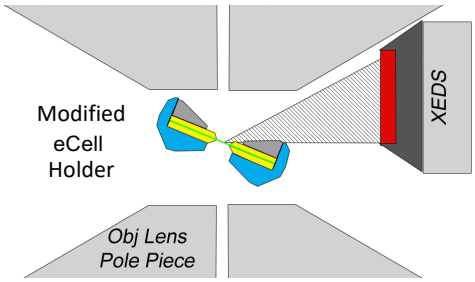

29

In-situ Cell (Liquid /Gaseous) Holders

Example: Protochips - Poseiden/Atmosphere Holder

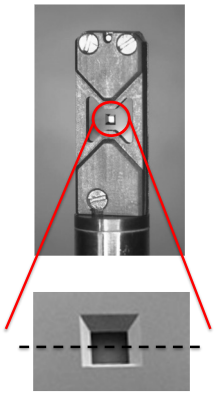

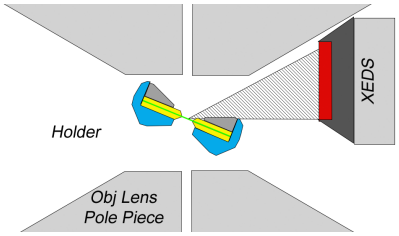

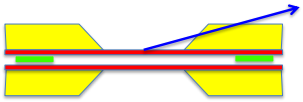

In-situ holders : FEI, JEOL, Hitachi, Gatan, Protochips, Hummingbird, DENsolutions,..

30

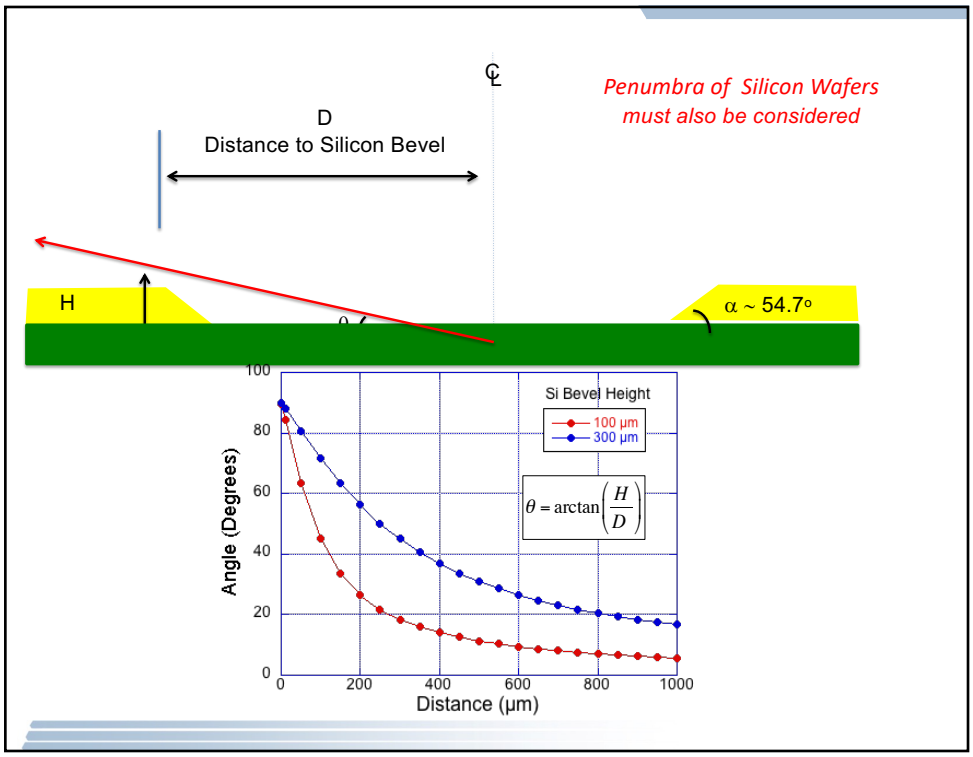
Penumbra of Silicon Wafers
must also be considered
D
Distance to Silicon Bevel
H
α ~ 54.7°
Si Bevel Height
100 µm
300 µm
$\theta = \arctan\left(\frac{H}{D}\right)$
Angle (Degrees)
Distance (µm)
0
20
40
60
80
100
0
200
400
600
800
1000

31

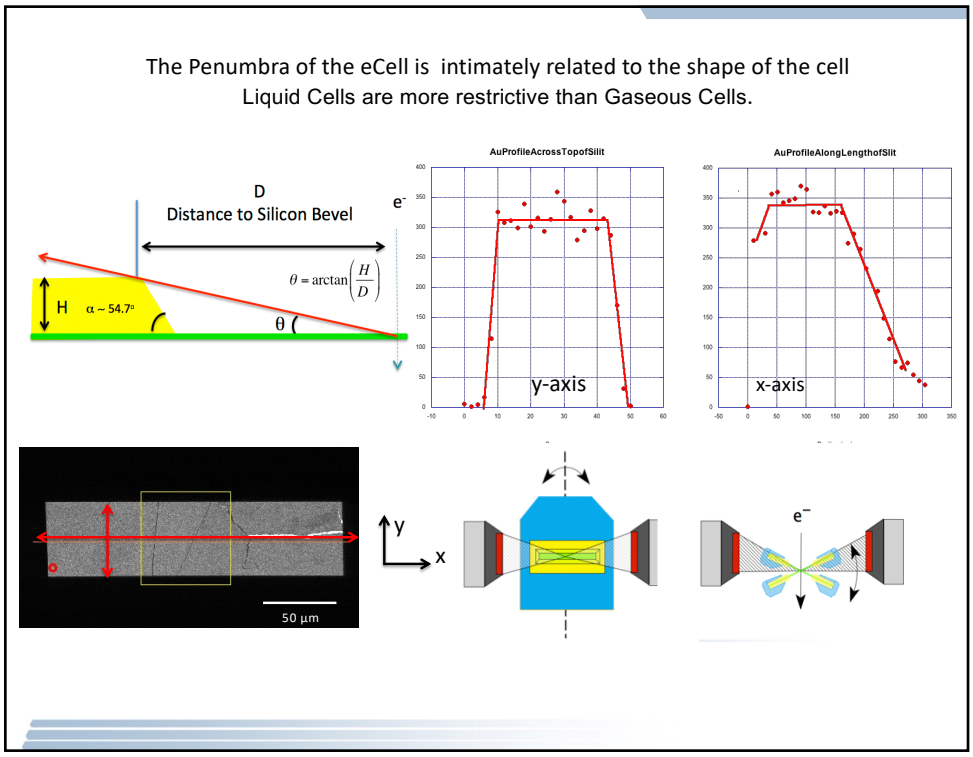
The Penumbra of the eCell is intimately related to the shape of the cell
Liquid Cells are more restrictive than Gaseous Cells.
D
Distance to Silicon Bevel
$\theta = \arctan\left(\frac{H}{D}\right)$
H
α ~ 54.7°
θ
e⁻
AuProfileAcrossTopofSilit
y-axis
AuProfileAlongLengthofSlit
x-axis
50 µm
y
x
e⁻

32

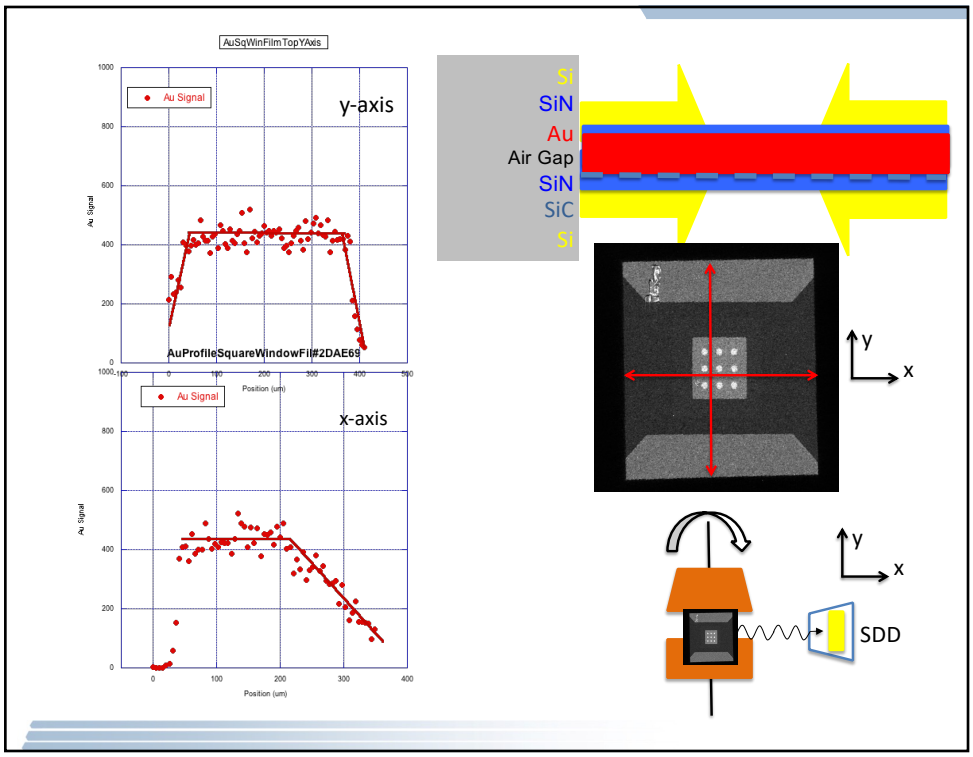
AuSqWinFilmTopYAxis
Au Signal
y-axis
AuProfileSquareWindowFil#2DAE69
Au Signal
x-axis
Position (um)
Si
SiN
Au
Air Gap
SiN
SiC
Si
y
x
y
x
SDD

33

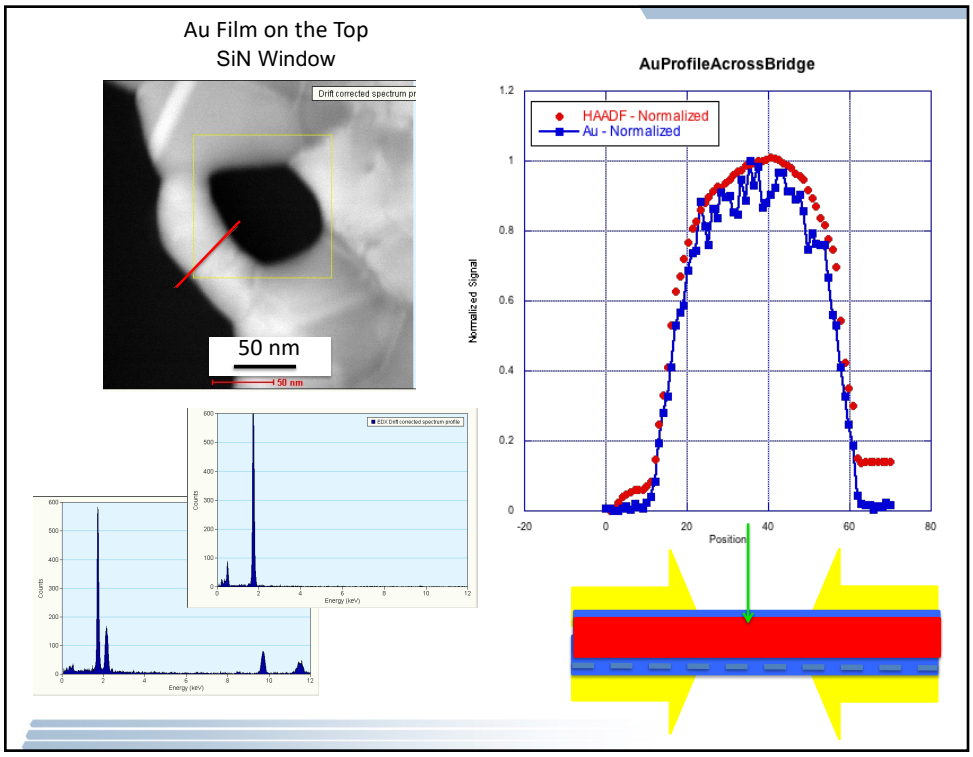
Au Film on the Top
SiN Window
50 nm
AuProfileAcrossBridge
HAADF - Normalized
Au - Normalized
Normalized Signal
Position

34

Au Film on the Bottom
SiN Window ***5 μm*** Gap

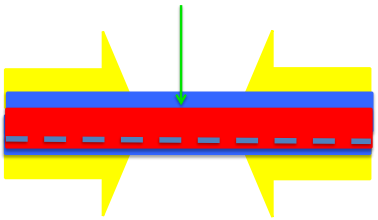

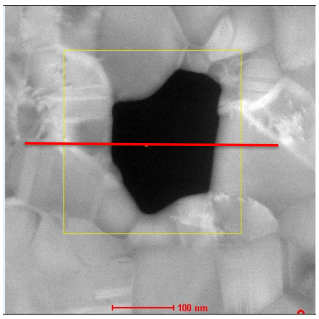

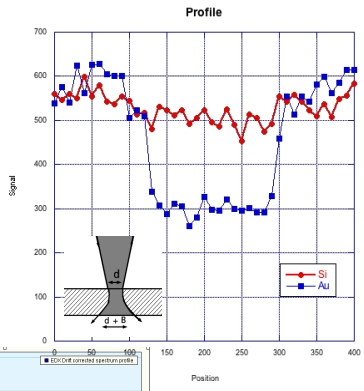

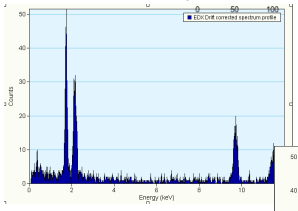

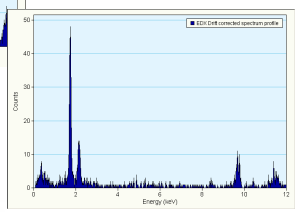

35

Gas Cell eChip Penumbra Measurements
Translation Series , Measurement at 20^0 holder tilt
Au Film on Top SiN Window with 1 Atm Air in the Gap

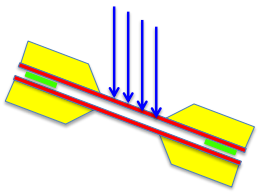

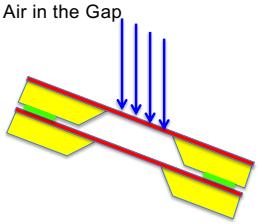

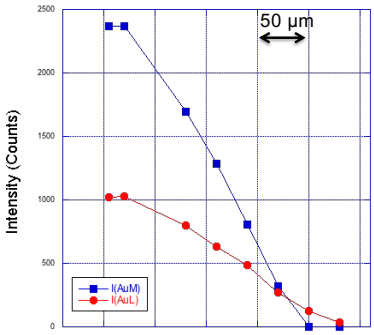

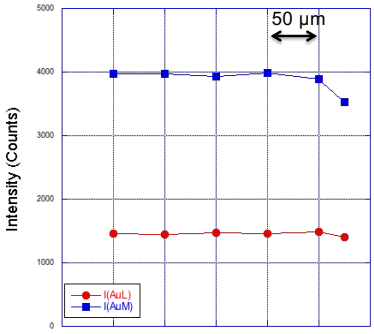

Standard Chip Assembly
Bevel “up”

Inverted Chip Assembly
Bevel “down”

36

Modeling X-ray Absorption in eCell System Windows and Media

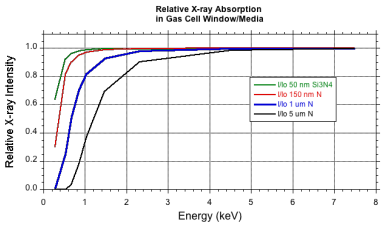

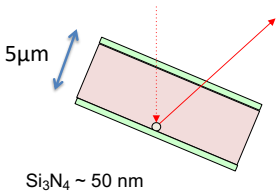

Si_3N_4 ~ 50 nm

N ~ 1000 nm (1 µm) @ 1 atm

Line	Energy (keV)	µ/ρ @ Si_3N_4 ρ ~ 1.33	µ/ρ @ N ρ ~ 0.81	I/Io in Si_3N_4 t ~ 50 nm	I/Io in N t ~ 150 nm	I/Io in N t ~ 1 µm	I/Io in N t ~ 5 µm
Ni Kα	7.48	48.64	9.25	0.9997	0.9999	0.9993	0.9963
Ti Kα	4.51	197.3	38.6	0.9987	0.9995	0.9969	0.9845
S Kα	2.31	1267.1	257.7	0.9916	0.9969	0.9793	0.9009
Al Kα	1.48	655.2	893.3	0.9957	0.9892	0.9302	0.6964
Na Kα	1.041	1767.5	2449.6	0.9883	0.9707	0.8200	0.3708
Ne Kα	0.851	3143.4	4372.7	0.9793	0.9483	0.7017	0.1702
F Kα	0.677	5878.2	8271.3	0.9617	0.9044	0.5117	0.0351
O Kα	0.52	12064.9	17191.5	0.9229	0.8115	0.2485	0.0009
C Kα	0.28	67557	98933	0.6381	0.3006	0.0042	0.0001

37

Prototype XEDS Gas Cell Chips – 2x50 nm SiN Window with SiC Heater ~ 5um Gap Air @ 50° C

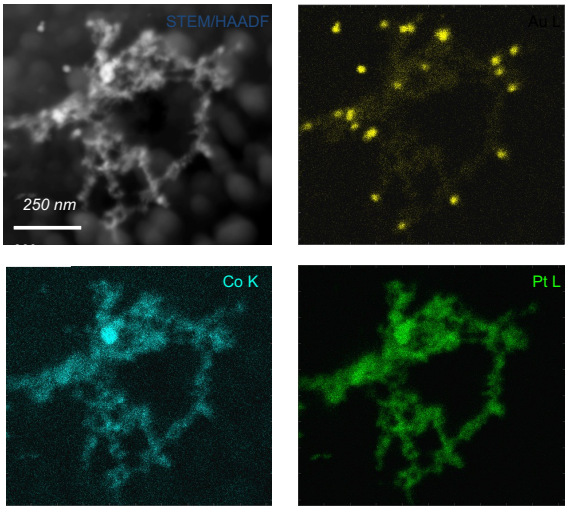

PtCo catalyst on Graphite Support on SiN/SiC window with 30 nm Au NP Anchors

Ref: 2015011901

38

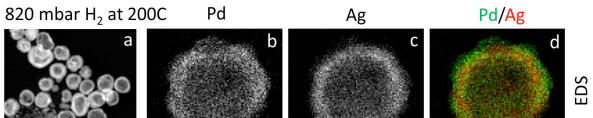

PdAg nanoparticles on SiNx

E_o = 200 kV
i_o = 600 pA
t = 20msec/pixel
t/λ ~ 0.8 @ SiNx

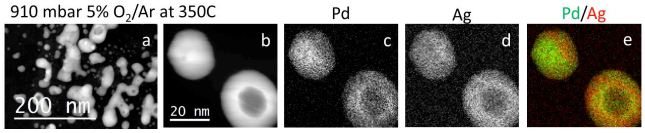

Prestat etal MM2015

39

In situ hyperspectral imaging of $FeTiO_3$ during reduction

In situ imaging and EDS of $FeTiO_3$ is during reduction reveled important aspects of the reduction process relevant to chemical looping combustion.

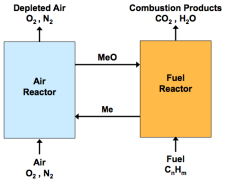

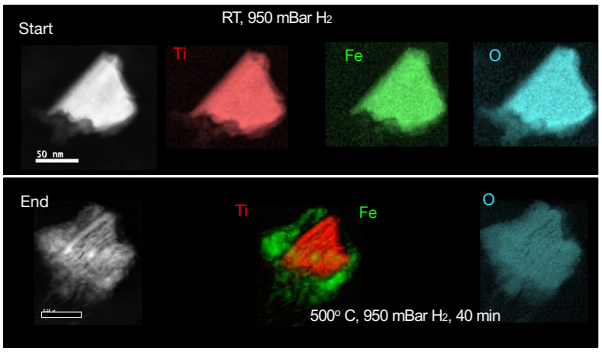

In situ hyperspectral imaging reveals:

- pseudomorphic reaction - shape of initial grains generally retained
- decomposition of $FeTiO_3$ to Ti-O and Fe-O

40

A.Janssen, et al.,
Microscopy & Microanalysis 2015 21 Sup 3 565-566

40

In situ hyperspectral imaging of $PdCu/TiO_2$ during H_2 reduction

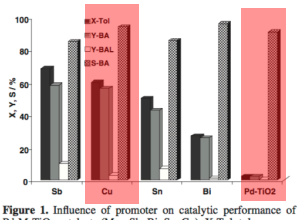

Figure 1. Influence of promoter on catalytic performance of Pd-M-TiO_2 catalysts (M = Sb, Bi, Sn, Cu); X-Tol: toluene conversion, Y-BA: benzyl acetate yield, Y-BAL: benzaldehyde yield, S-BA: benzyl acetate selectivity.

- Understanding the chemical changes during oxidation/reduction is important in many processes.
- Supported bi-metal nanoparticle catalysts are key materials for diverse conversion processes throughout chemical industries.
- Bimetallic catalysts frequently offer improvements in activity, selectivity, and stability compared to their monometallic equivalents for diverse reactions such as catalytic reforming, hydrotreating, emissions controls, and biomass conversion.
- Evolution of catalyst microstructure and composition is of significant interest due to its role in understanding processing.

Models of PdCu Catalysts

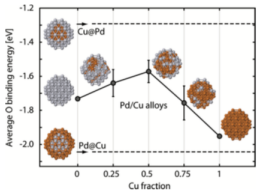

Tang etal. J. Phys. Chem. Lett. 2011, 2, 1328–1331

41

Pd Cu on TiO_2

PdCu catalyst is representative of a large group of bimetallic catalysts useful for a range of chemical conversions including catalytic reforming, hydrotreating, emissions controls, and biomass conversion.

Studied at:
~ 1 ATM of Air & H_2
RT->550°C

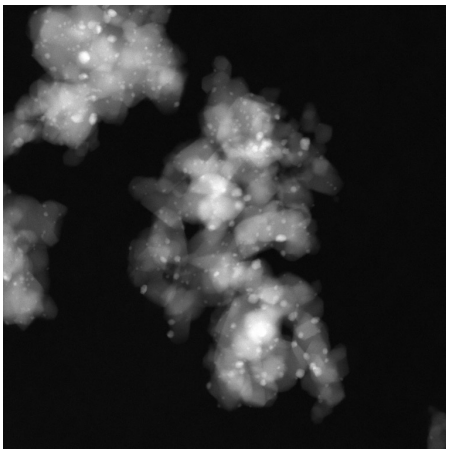

M. A. Kulzick, P. J. Dietrich, E. Prestat, M. Smith, M. G. Burke, S.J. Haigh N.J. Zaluzec

42

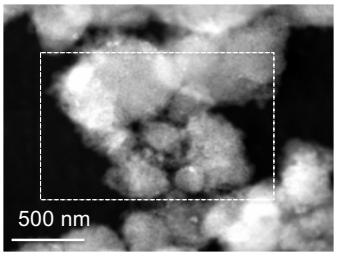

Pd/Cu NP Catalysts on TiO_2
Calcined vs Reduced
In-situ Gas Reaction Cell
0.7 atm H_2

Same Area Pre/Post Temp
Note Cu changes

RT H_2

Post 500°C H_2

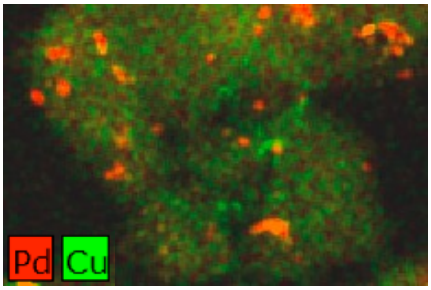

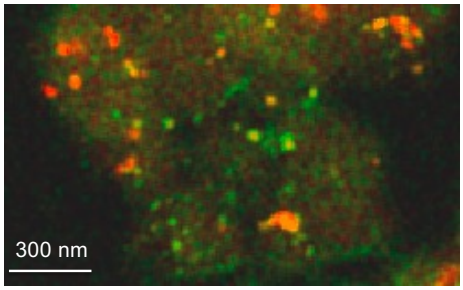

2014100105 -> 28

43

EX SITU STEM ANALYSIS OF PdCu/TiO_2 CATALYSTS

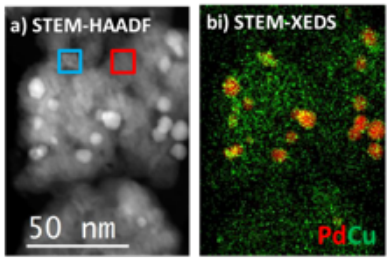

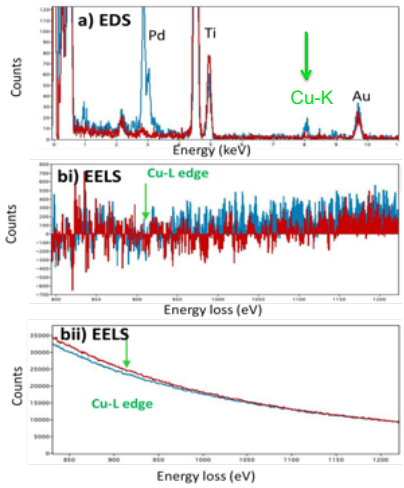

44

Traditional Catalyst Characterization
In-Situ
XANES Measurements
CuK and Pd K
1 Atm @ Temp

Sector 10 MRCAT
ANL APS

ANL Advanced Photon Source

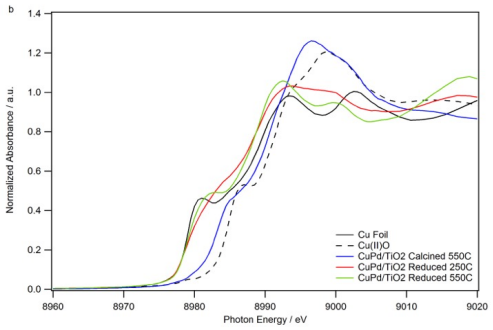

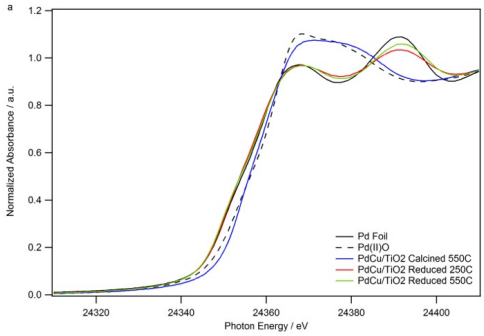

45

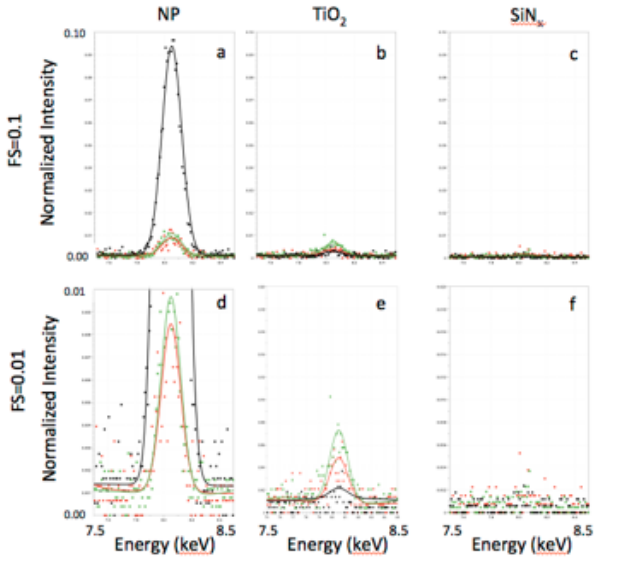

Cu Np's increase with Temp

Cu on TiO2 decreases with increase Temp > 250 C

No discernable Cu on SiN with Temp

Normalized Copper Distributions Normalized

100 C
250 C
550 C

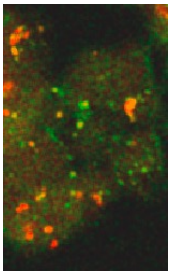

46

In situ XEDS @ ATM @ Temperature

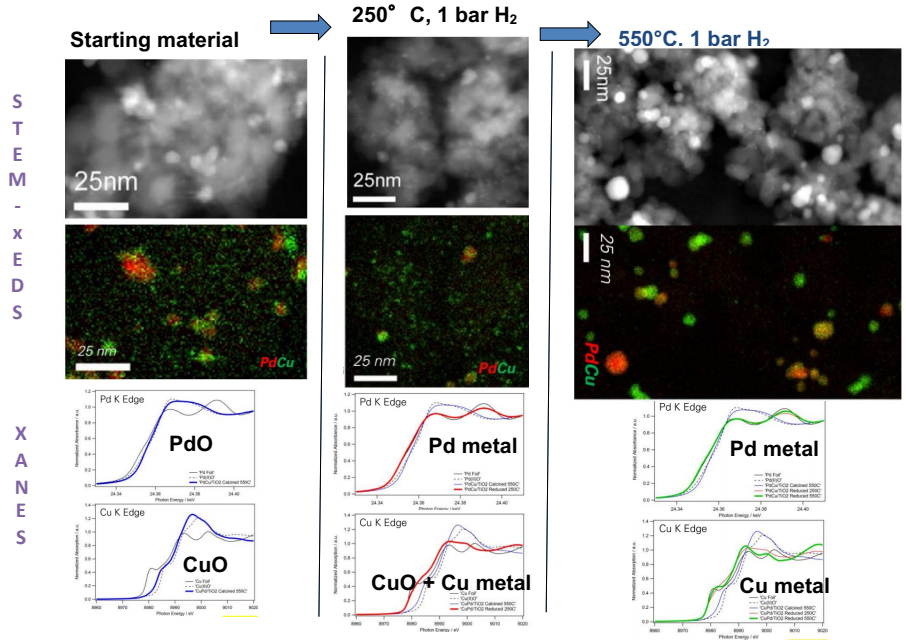

47

During dynamic in-situ experiments

spectroscopy can become essential to the interpretation

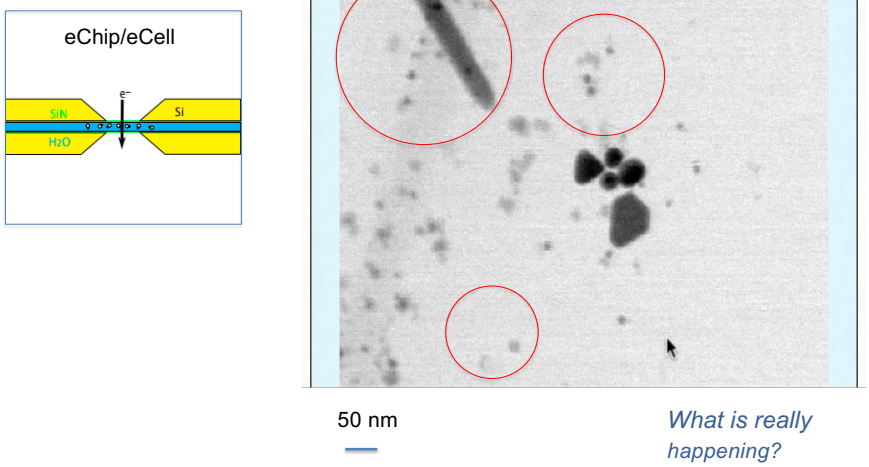

What is really happening?

48

Why XEDS ? Just use EELS!

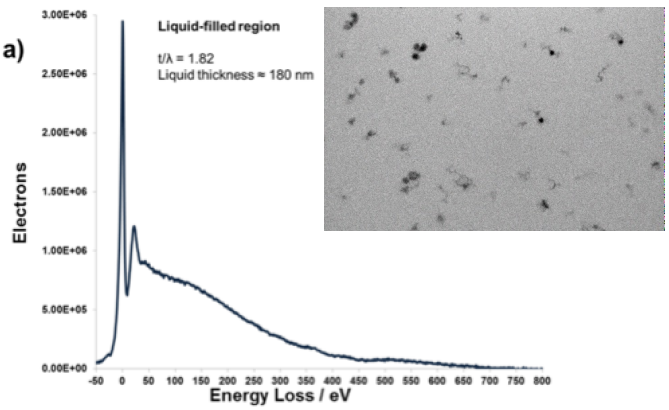

Gases are doable, but liquids are a real problem

49

In-situ cells with SiNx windows, thick materials and media become problematic for spectroscopy. This can dictate the spectroscopic methodology

Simultaneous XEDS/EELS

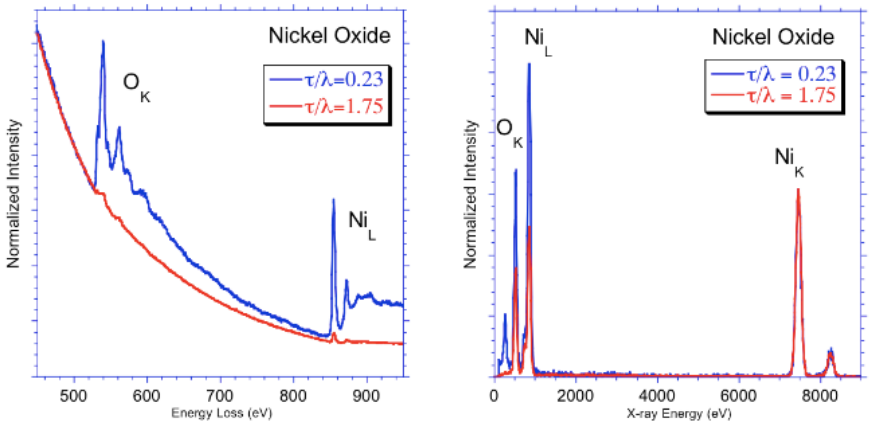

XEDS has a real advantage in thick "specimens"
Due to its improved performance wrt P/B
but there are geometrical collection solid angle issues

50

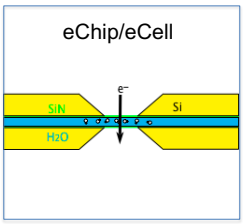

Spectroscopy in Liquid eCells

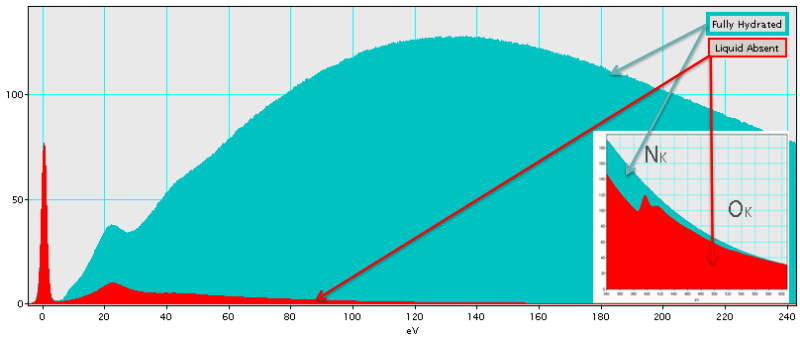

eCell Media Dominates EELS Signal

51

Compare Simultaneous EELS/XEDS
in eCell in H_2O

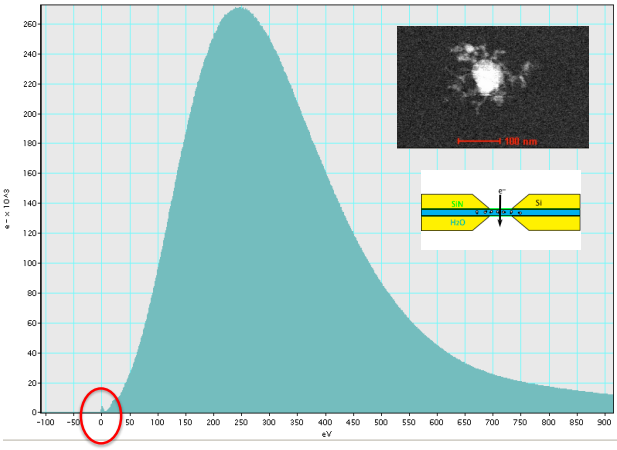

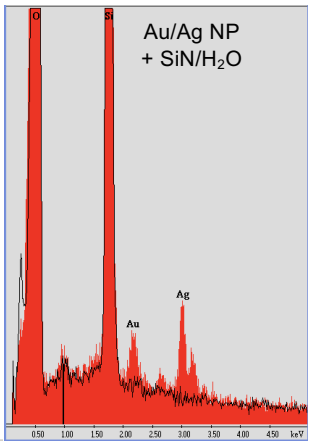

Simultaneous EELS/XEDS in Liquids
Multiple Scattering dominates EELS signal P/B is terrible
XEDS signal from the specimen not dominated by Bgnd
Si N, O are present from environmental media

52

XEDS of the "media" in the eCell

Can now also verify the presence and composition of the media

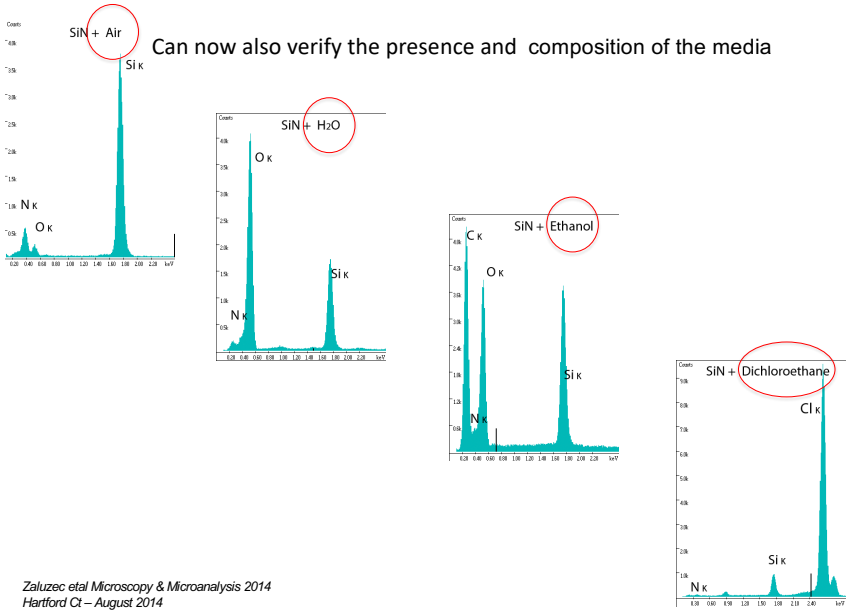

Zaluzec etal Microscopy & Microanalysis 2014
Hartford Ct – August 2014

53

Hyperspectral Imaging of Nanoparticle Soup in Liquids

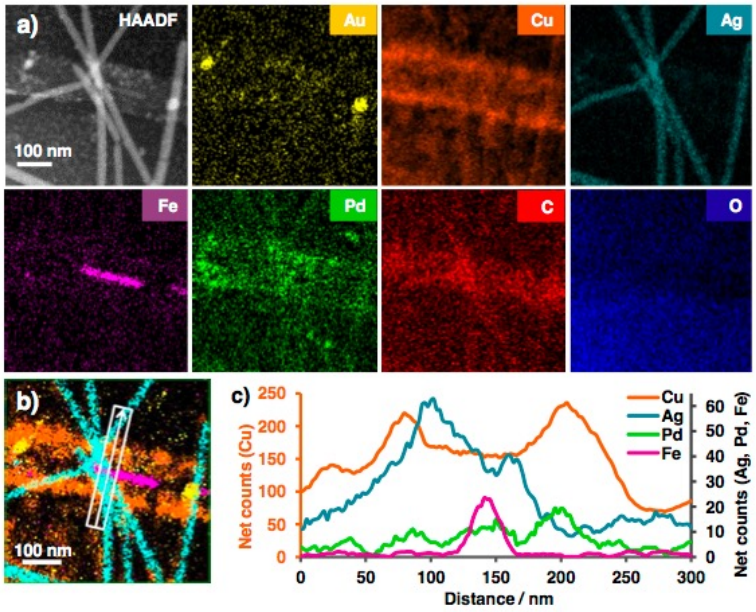

Lewis etal - Chem. Commun., 2014, 50, 10019

Spatial Resolution ~ 10-20 nm at present

54

After Modification/Optimization

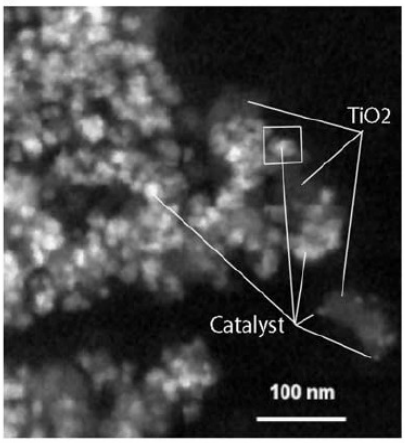

Pd/Sb/Mo catalyst
On TiO_2 support
in H_2O between
SiN Windows

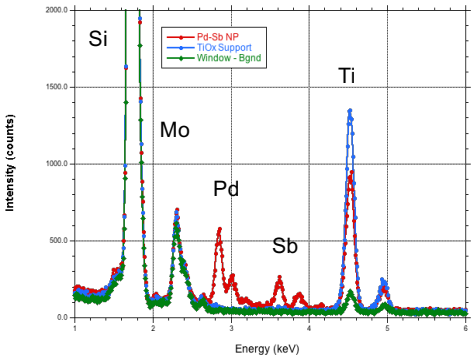

Zaluzec etal Microsc. Microanal. 20, 323–329, 2014
doi:10.1017/S1431927614000154

55

Xray Attenuation by
Various amounts of liquid cell
media and an SiN_x window

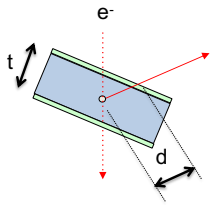

Line	Energy (keV)	μ/ρ @ Si_3N_4 ρ ~ 1.33	μ/ρ @ H_2O ρ ~ 1	I/Io in Si_3N_4 d ~ 50 nm	I/Io in H_2O d ~ 150 nm	I/Io in H_2O d ~ 500 nm	I/Io in H_2O d ~ 1 μm
Ni Kα	7.48	48.64	12.98	0.9997	0.9998	0.9994	0.9987
Ti Kα	4.51	197.3	56.22	0.9987	0.9992	0.9972	0.9944
S Kα	2.31	1267	390.6	0.9916	0.9942	0.9807	0.9617
Al Kα	1.48	655.2	1418	0.9957	0.9789	0.9315	0.8677
Na Kα	1.041	1767	3943	0.9883	0.9426	0.8211	0.6742
Ne Kα	0.851	3143	7050	0.9793	0.8997	0.7029	0.4941
F Kα	0.677	5878	13678	0.9617	0.8145	0.5046	0.2547
O Kα	0.52	12064	29376	0.9229	0.6436	0.2302	0.0530
C Kα	0.28	67557	176560	0.6381	0.0707	0.0001	0.00000001

Calculation of x-ray absorption as a function of pathlength for a range of characteristic x-ray lines in SiN_x window and various amounts of liquid H_2O. As I/Io approaches unity the effects of x-ray absorption can be ignored.

56

Limitations of liquid environmental TEM studies

- Electron scattering by liquid
- Sample preparation
- Mostly limited to materials such as nanoparticles or nanowires

"Bulk" metals/alloys in liquid environment studies?

- Preparation of suitable metal specimens – challenging
- Dimensional requirements for the liquid *in situ* eCell

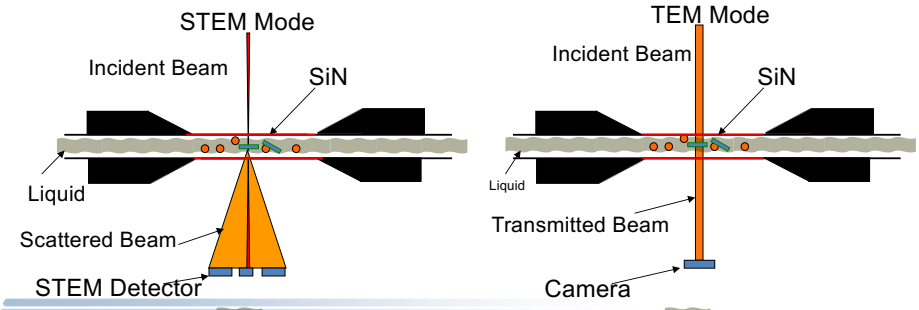

57

Hybrid Specimen Preparation Methods to Study Conventional Materials

'Cut-and-Paste' approach using Dual Beam FIB

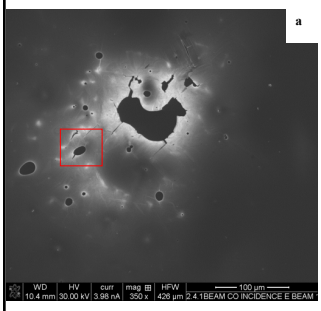

Quanta 3D DF-STEM image

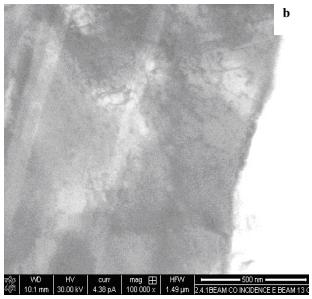

BF-STEM image

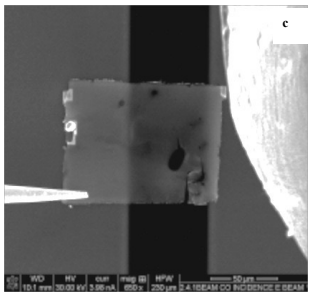

"cut" sample placed on TEM liquid cell window (50 μm wide)

58

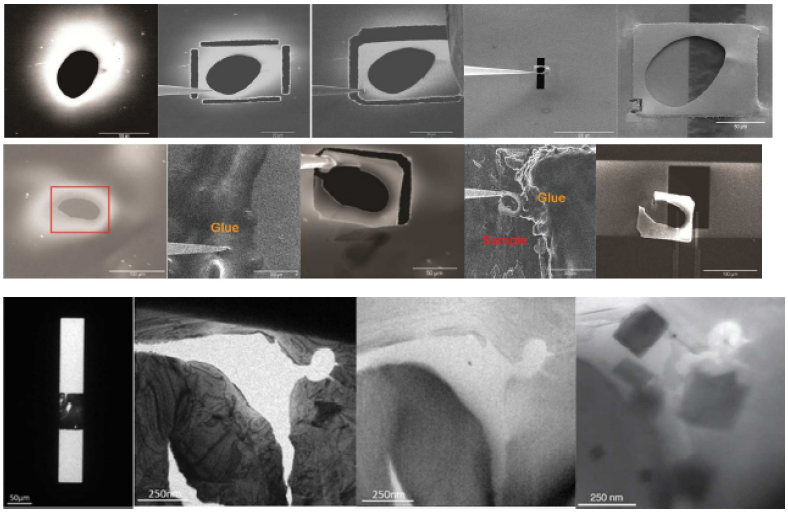

59

The “media” also affects the imaging

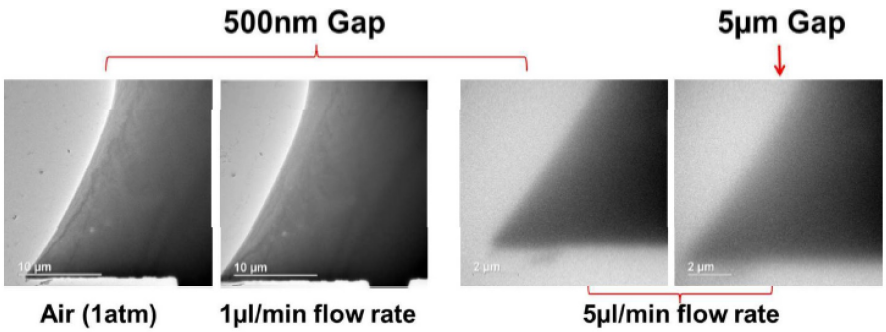

60

FIB section of 304 Steel positioned over SiN Window in 5 µm eCell

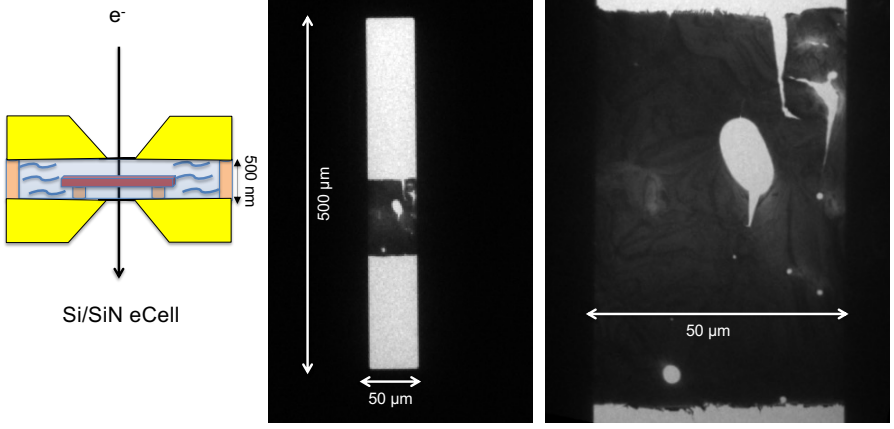

Figure 14 Illustration of the use of TEM and FIB/SEM to prepare and mount
An electropolished specimen into a liquid cell for combined XEDS/corrosion studies

61

Spectrum Imaging
Type 304 Austenitic Stainless Steel in Water

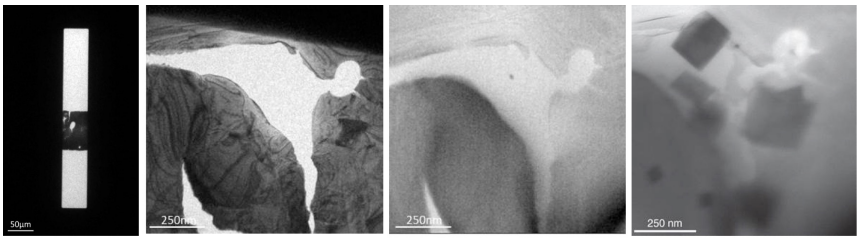

1 Atm Air | 1 Atm H_2O | 1 Atm H_2O + 24 hrs

62

Spectrum Imaging
Type 304 Austenitic Stainless Steel in Water

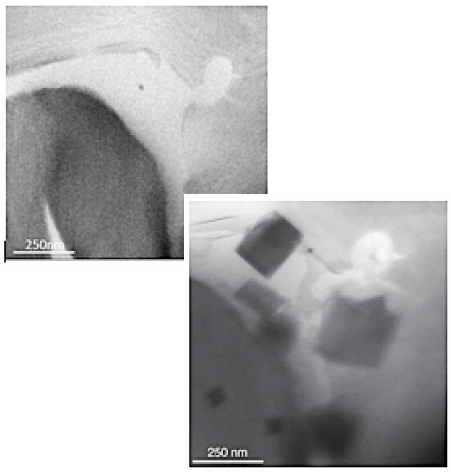

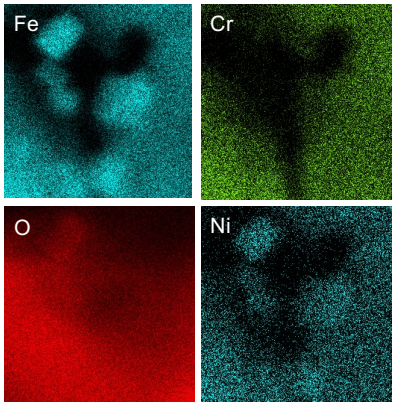

Microstructural Evolution in Liquid H_2O

Note absence of Cr in the Precipitates formed after emersion in H_2O ~ 24 hrs.

63

MnS Ppt in Steel

Dissolution in H_2O

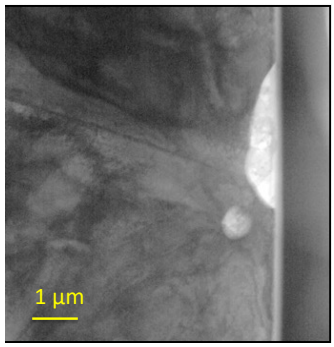

Dry

Dry

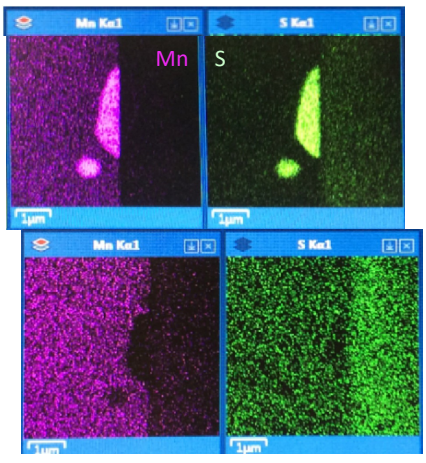

Wet

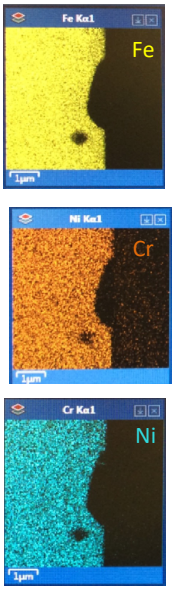

64

Electrochemical Studies add yet additional factors

1.) Electrode Configurations

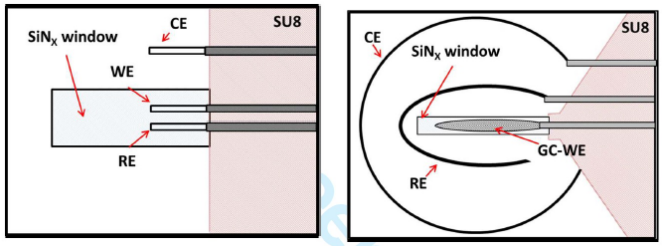

1.) Electrode Connections

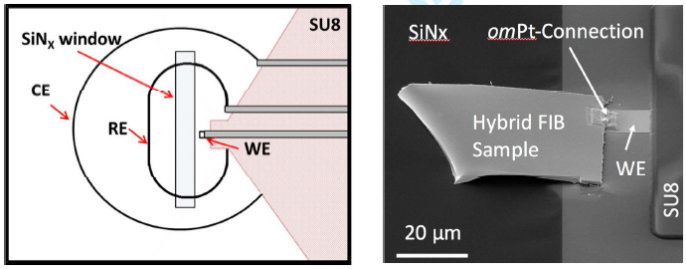

65

Hybrid Prep Also Important for ElectroChemical Studies

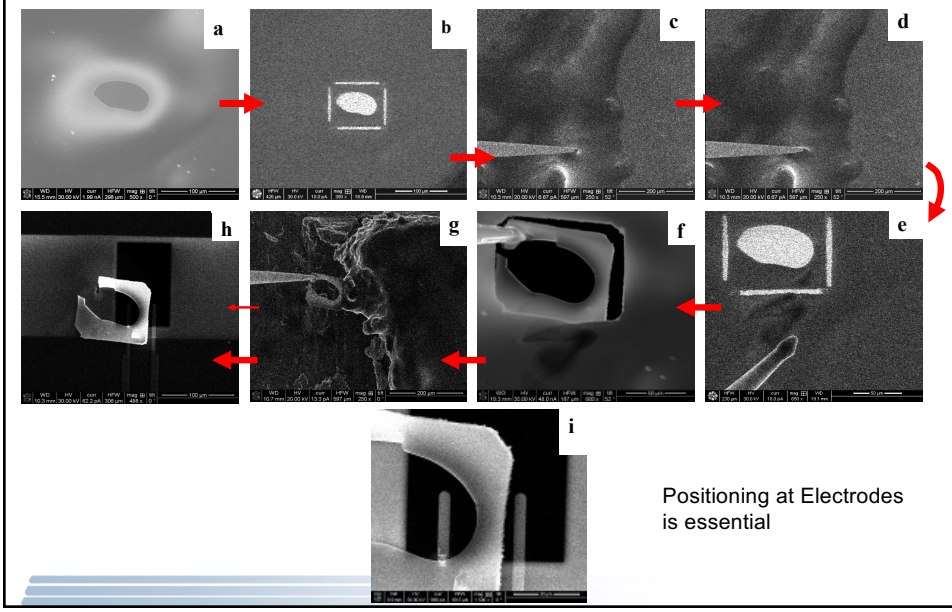

Positioning at Electrodes is essential

66

Beam induced issues must be identified

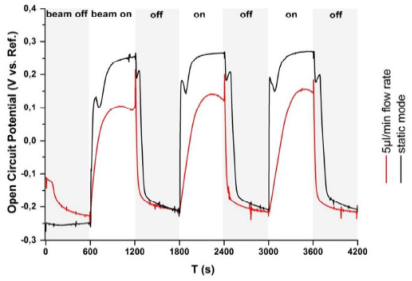

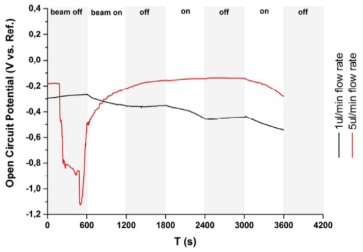

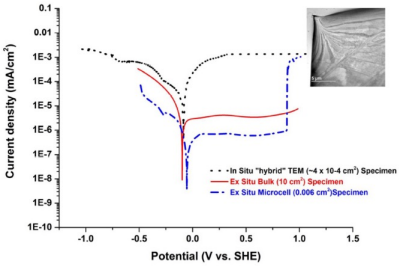

Practical Aspects of Electrochemical Corrosion Measurements During In Situ Analytical Transmission Electron Microscopy (TEM) of Austenitic Stainless Steel in Aqueous Media.
Microsc Microanal. 2017 Aug;23(4):741-750. doi: 10.1017/S1431927617012314.
Schilling etal

67

Hydrated electrons ??

In all microscopy experiments, the electron beam interacts with the sample resulting in the generation of radical and molecular species, which for water include e^h (hydrated electrons), OH, H^+, H_2, O_2, and H_2O_2. The hydrated electrons, oxidizing agents, and gaseous species can cause, respectively, reduction and precipitation of cations from solution, dissolution of metals, and nucleation and growth of bubbles.

e^- (aq) + H_2O——> H + OH^-
e^- (aq) + H^+ ——> H

The hydrated electron can act as a reducing agent.
For example:

Cu^{2+} + e^- (aq)——> Cu^+
[Cu^{2+} + H------> Cu^+ + H^+]

Alot of work is still needed to understand and correctly measure and interpret all liquid TEM/STEM experiments.

68

Why was in situ Correlative Important?

- *We can observe different details*
  - *Reveals nanometer scale concentration changes*
  - *But details not apparent without high resolution*
- *XANES invaluable but needed supplemental info*
- *XEDS saw all the critical elements*
  - *EELS is valuable , but not applicable here*
- *We can localize specific areas*
  - *In complex materials this is very important*
  - *Thermal drift adds complexity*
- *Beware beam induced changes!*

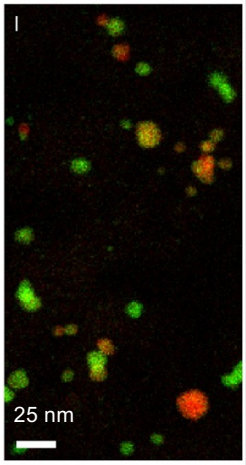

69

69

STEM + XEDS tomography

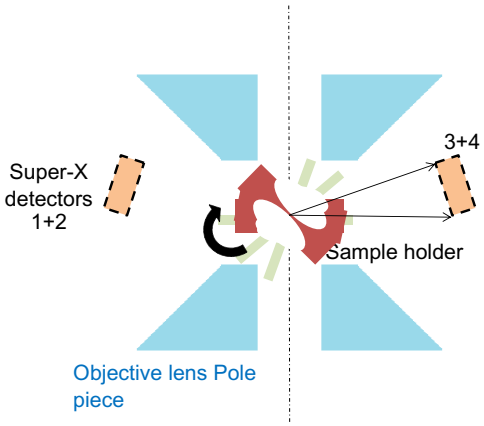

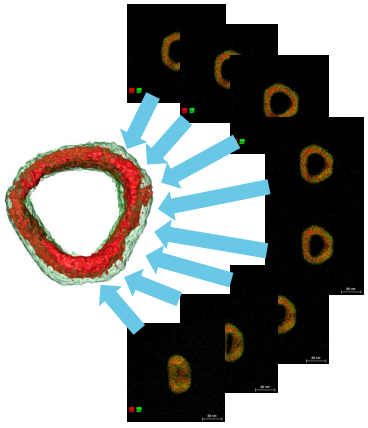

70

71

III-Nitride Nanopyramid LED

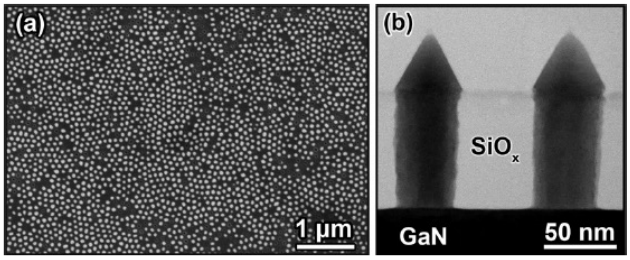

Plan-view FESEM of a GaN seed nanorod array selectively grown through a dielectric template. (b) Bright-field STEM cross-section of two typical GaN seed nanorods (grown at 1030° C) with faceted pyramidal caps protruding above the dielectric template.

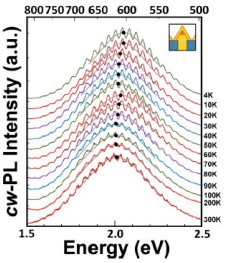

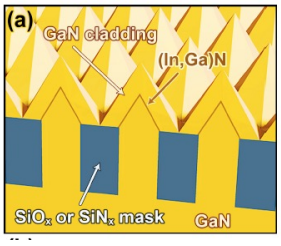

Wildeson etal. JOURNAL OF APPLIED PHYSICS 108, 044303 2010

72

Electron Tomographic Data Acquisition

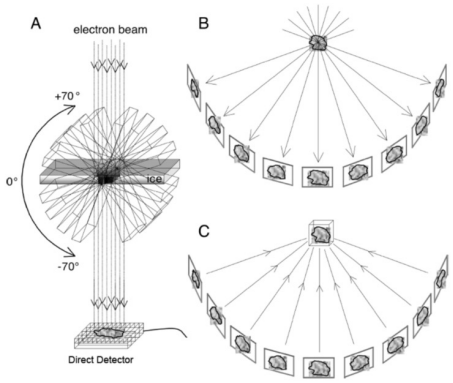

Steven and Belnap, Current Protocols in Protein Science, 2005

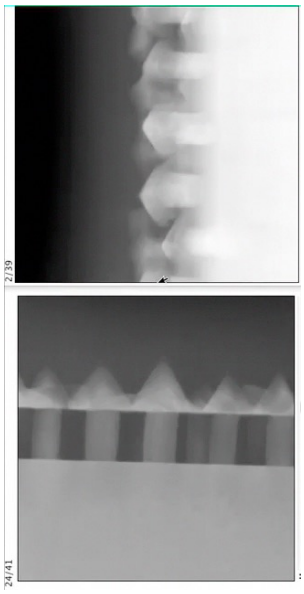

1K x 1K Hyperspectral Images
± 60⁰ @3⁰ increments dual axis tilt series

Alignment via cross-correlation Reconstruction via SIRT

73

STEM Tomography

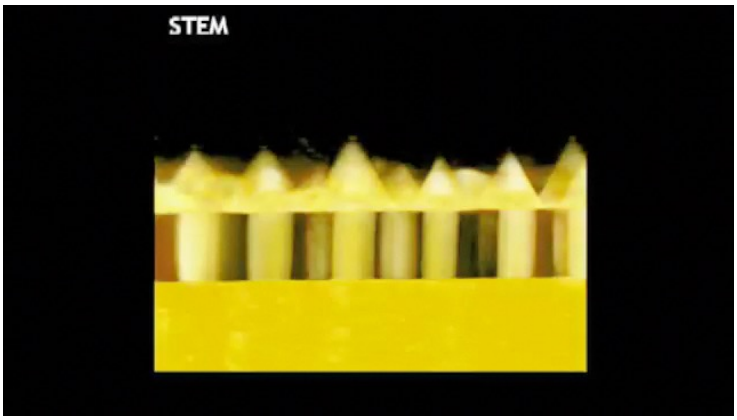

74

HyperSpectral Imaging is limited by Data Acquisition TIME

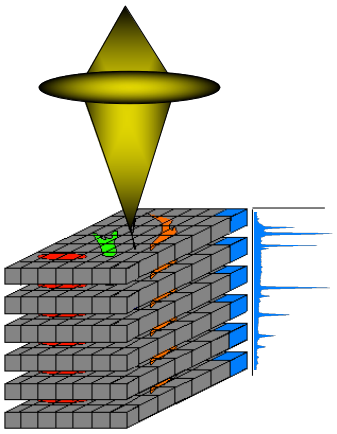

⇒ Collect the signal as efficiently as possible

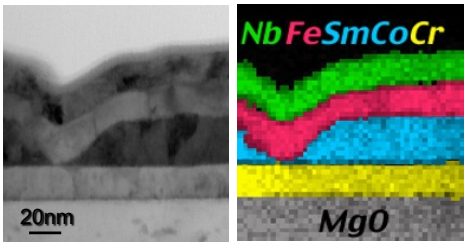

t / XY	1 µs	1 ms	1 s	10 s
512^2	0.26 s	4.3 min	3 dy	1 mnth
1024^2	1 s	17.5 min	12.1 dy	4 mnth
4096^2	16 s	4.6 hrs	6.4 mnth	5.3 yrs

75

STEM Tomography -> Hyperspectral Imaging Tomography

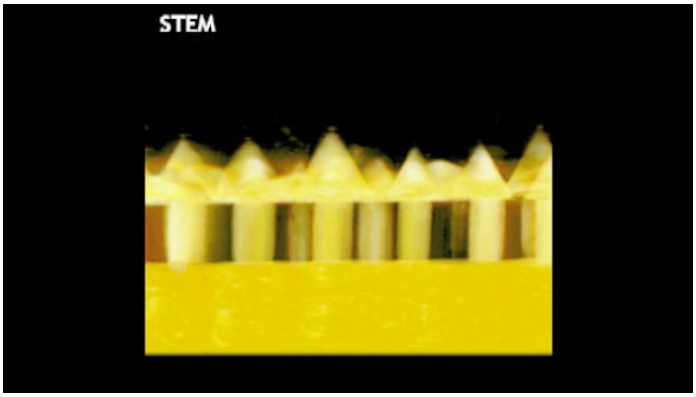

Tomographic reconstruction using Inspect 3D
1K x 1K Hyperspectral Images
HAADF, Ga_K, In_L, N_K, Si_K
$\pm 60^0$ @ 3^0 increments dual axis tilt series
5 minutes / frame ~ 7 hrs ~ 20 Gb
200 kV, 1 nA @ 160kX
FIB X-section & Plasma Cleaned !

76

Are tomography assumptions valid for XEDS?

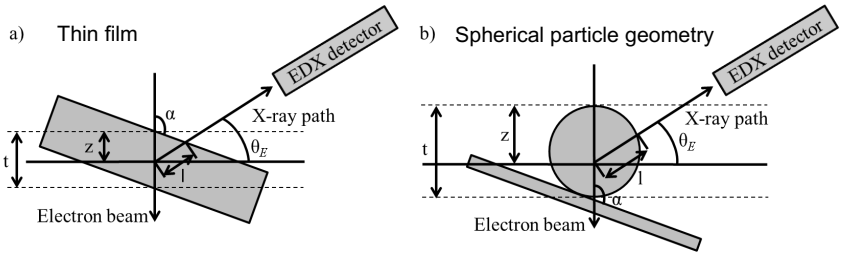

Absorption correction factor for spherical particle geometry with beam in centre

$$ACF = \frac{\int_0^{2R} e^{\left[\frac{\mu}{\rho}\right]^B \rho\left(\sqrt{R^2-((z-R)\cos\theta_E)^2}-(R-z)\sin\theta_E\right)} dz}{\int_0^{2R} e^{\left[\frac{\mu}{\rho}\right]^A \rho\left(\sqrt{R^2-((z-R)\cos\theta_E)^2}-(R-z)\sin\theta_E\right)} dz}$$

α = beam incidence angle
θ_E = elevation angle
μ/ρ = mass attenuation coefficient
t = thickness
R = particle radius
A,B = elements

- Neglecting absorption is valid for particles smaller than 160nm in diameter when considering high energy X-ray peaks

N. Zaluzec *Microbeam Anal (San Francisco)*, 167, 1981

TJA Slater, Y Chen, G Auton, NJ Zaluzec, SJ Haigh;, Microscopy and Microanalysis 2016 in press

77

Intensity Variation Multi-axis Detectors & Holders

Low background double tilt holder

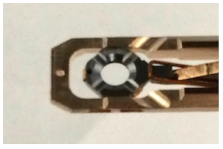

2020 Fischione tomography holder

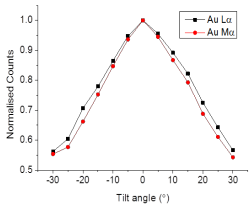

b)

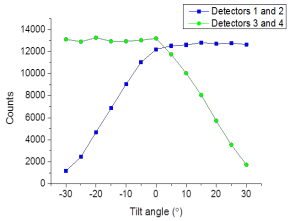

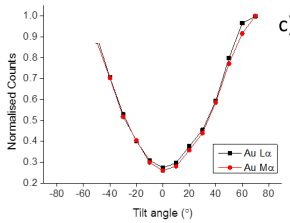

c)

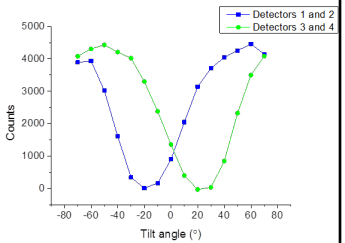

T. Slater. et al EMAG 2014

Slater, Janssen, Camargo, Burke, Zaluzec· Haigh, Ultramicroscopy 162, 61, 2016

78

Are XEDS tomo assumptions valid?

Optical profiles of the top and bottom surfaces of the Fischione 2020 holder.

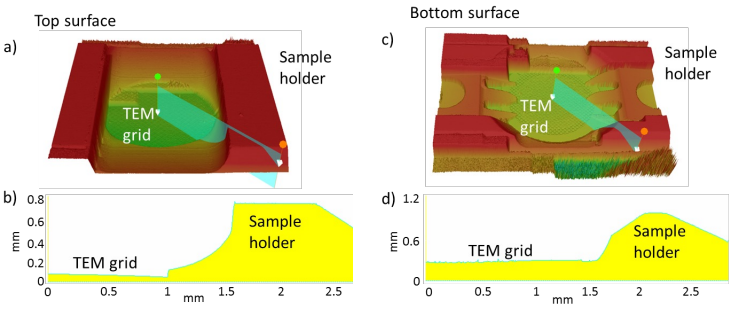

- Shadowing polar angle of 21° and 18° from the centre of the grid to the highest point of the top and bottom surfaces of the holder
- However 200mesh Cu support grid shadows for angles of 0° above and 24° below

Slater, Janssen, Camargo, Burke, Zaluzec, Haigh, Ultramicroscopy 162, 61, 2016

79

Why do you need constant intensity?

- Demonstration of potential artefacts associated with variations in projection intensities.

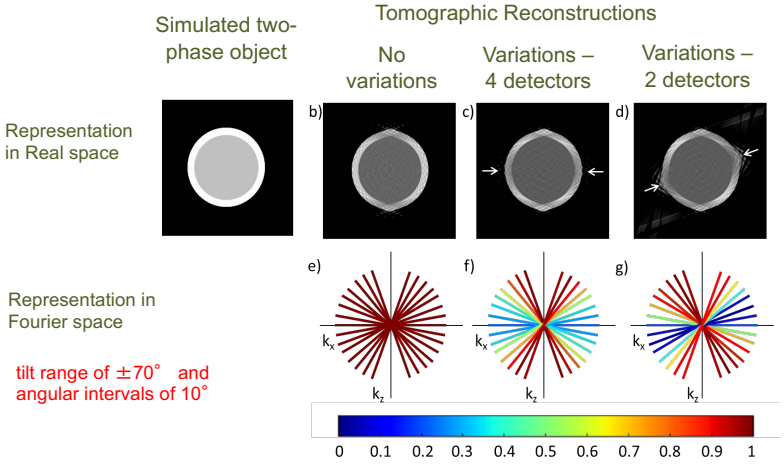

Slater, Janssen, Camargo, Burke, Zaluzec, Haigh, Ultramicroscopy 162, 61, 2016

80

Estimating elemental surface segregation from 2D XEDS map

Au XEDS map

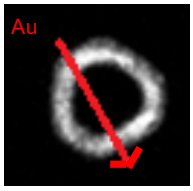

Ag XEDS map

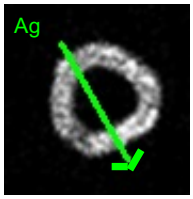

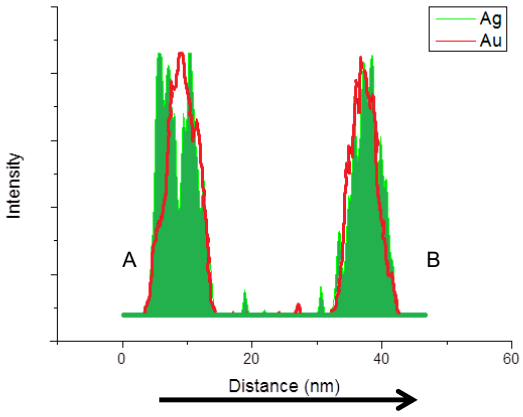

T. Slater. et al Nanoletters 2014

81

Time varied tomographic acquisition for compensation of detector shadowing

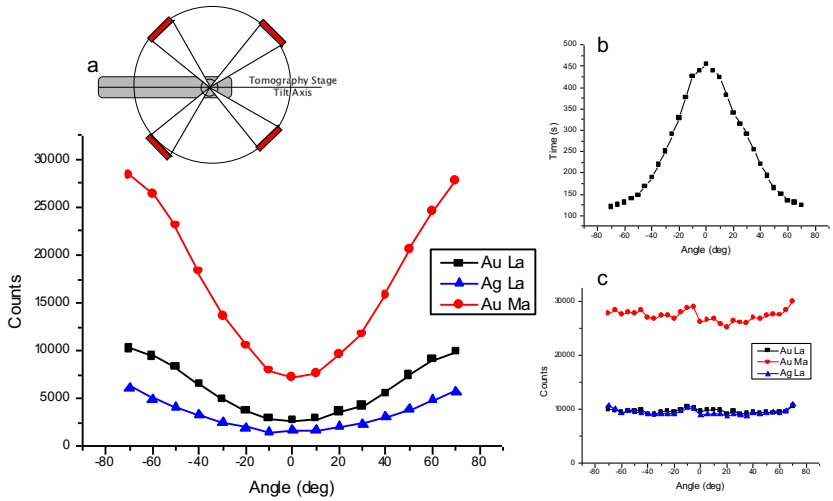

Tilt-dependent acquisition times mean signal counts are effectively constant ±15% for all tilt angles

Slater, Janssen, Camargo, Burke, Zaluzec, Haigh, Ultramicroscopy 162, 61, 2016

82

3D EDX elemental mapping at nanoscale

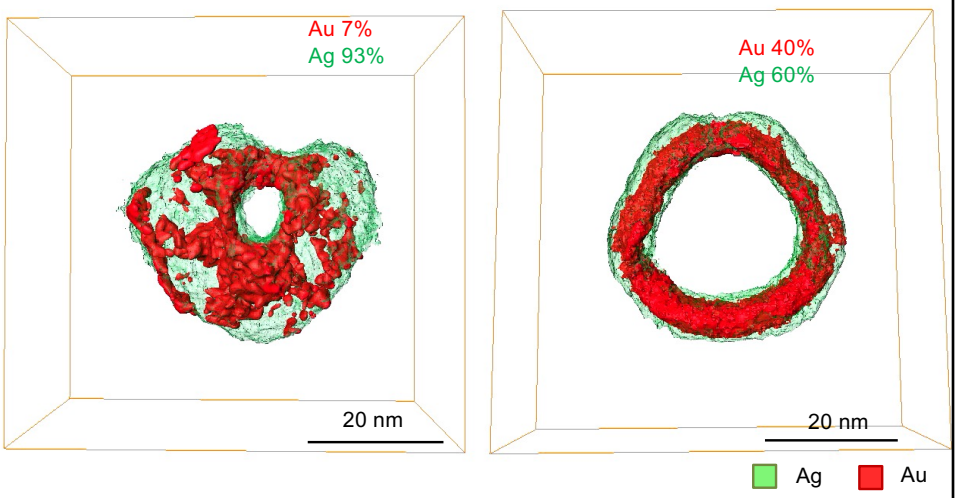

Slater et al. Nano Letters (2014)

83

1960 - Fuller and Hale

First Reported Imaging Magnetic Domains in TEM

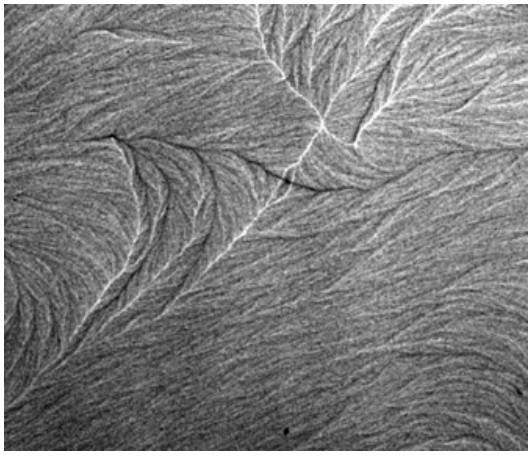

84

Lorentz Microscopy: Fresnel

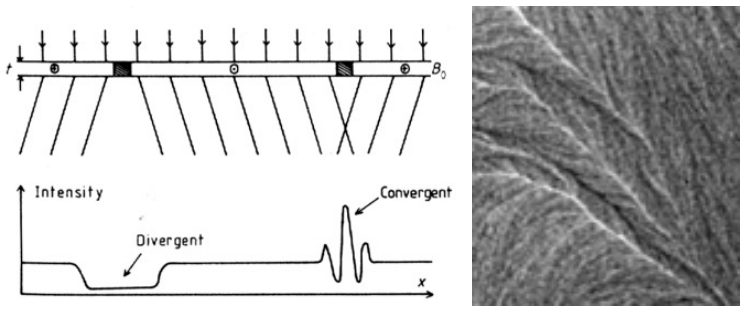

85

Lorentz Microscopy: Fresnel

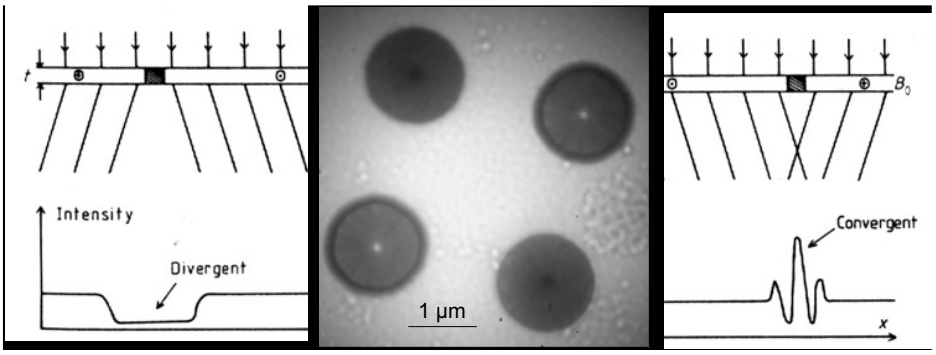

86

Lorentz Microscopy

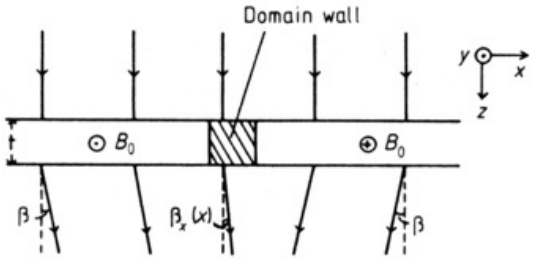

Fuller and Hale 1960

$$\beta = \frac{4\pi}{c}\left(\frac{e}{m}\right)\left(\frac{B_o t}{v}\right)$$

Eo	t=200 (nm) B=1000 (G)	t=200 (nm) B=5000 (G)
100 kV	0.22 mR	1.1 mR
200 kV	0.15 mR	0.75 mR
300 kV	0.12 mR	0.6 mR

87

Observing Controlled Vortex and Domain Motion

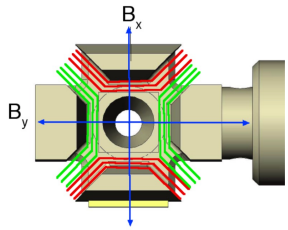

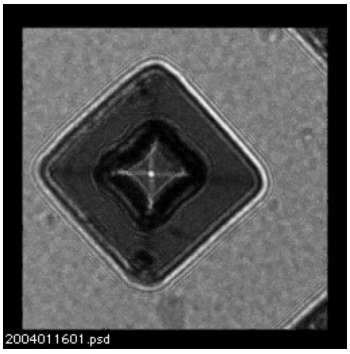

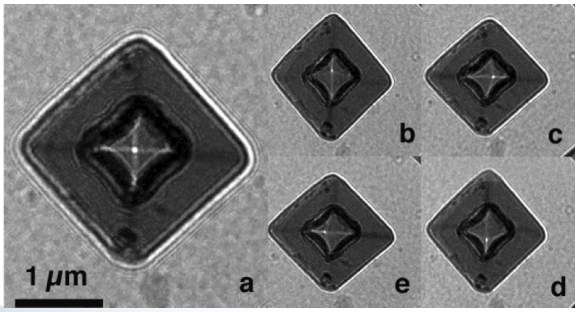

88

Lithographically Fabricated Permalloy Arrays

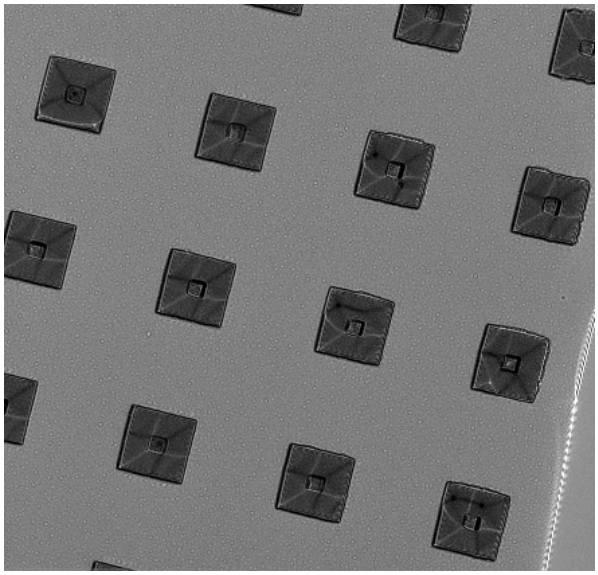

B

Magnetic states are not always uniform ==> Understanding individual elements is also important

89

Lithographically Fabricated Permalloy Arrays

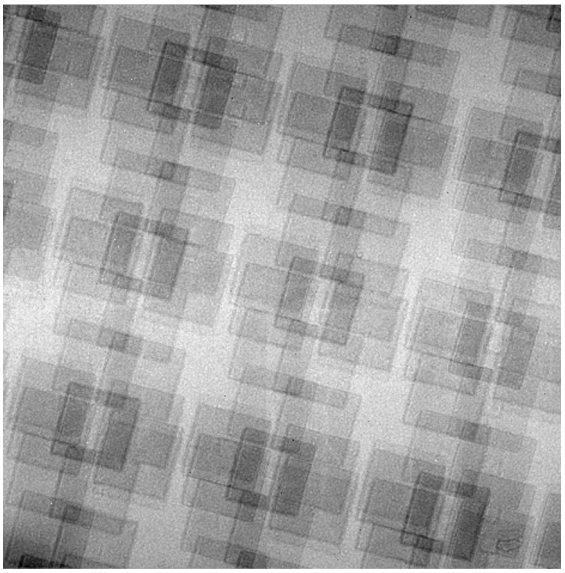

B

90

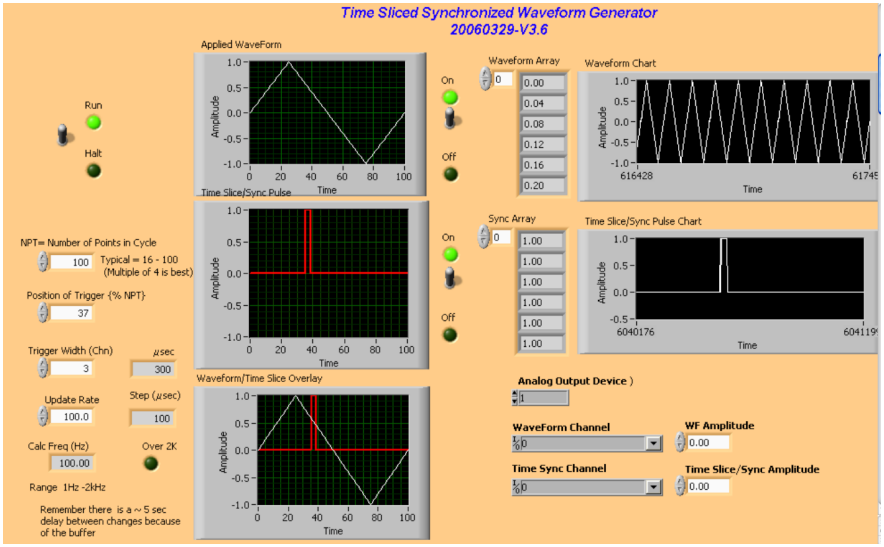
Time Sliced Synchronized Waveform Generator
20060329-V3.6
Applied WaveForm
Waveform Array
Waveform Chart
Run
Halt
On
Off
Time Slice/Sync Pulse
Sync Array
Time Slice/Sync Pulse Chart
NPT= Number of Points in Cycle
Typical = 16 - 100
(Multiple of 4 is best)
Position of Trigger {% NPT}
Trigger Width (Chn)
µsec
Update Rate
Step (µsec)
Calc Freq (Hz)
Over 2K
Range 1Hz -2kHz
Remember there is a ~ 5 sec
delay between changes because
of the buffer
Waveform/Time Slice Overlay
Analog Output Device)
WaveForm Channel
WF Amplitude
Time Sync Channel
Time Slice/Sync Amplitude
Amplitude
Time

91

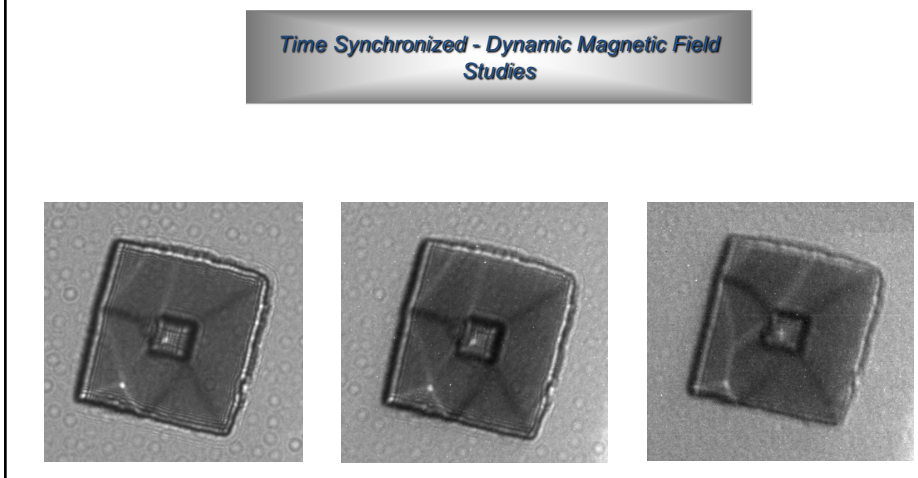
Time Synchronized - Dynamic Magnetic Field Studies
Static Field
Static Beam
Static Field
Synchronized Beam
500 µsec
Dynamic Field
Synchronized Beam
500 µsec

92

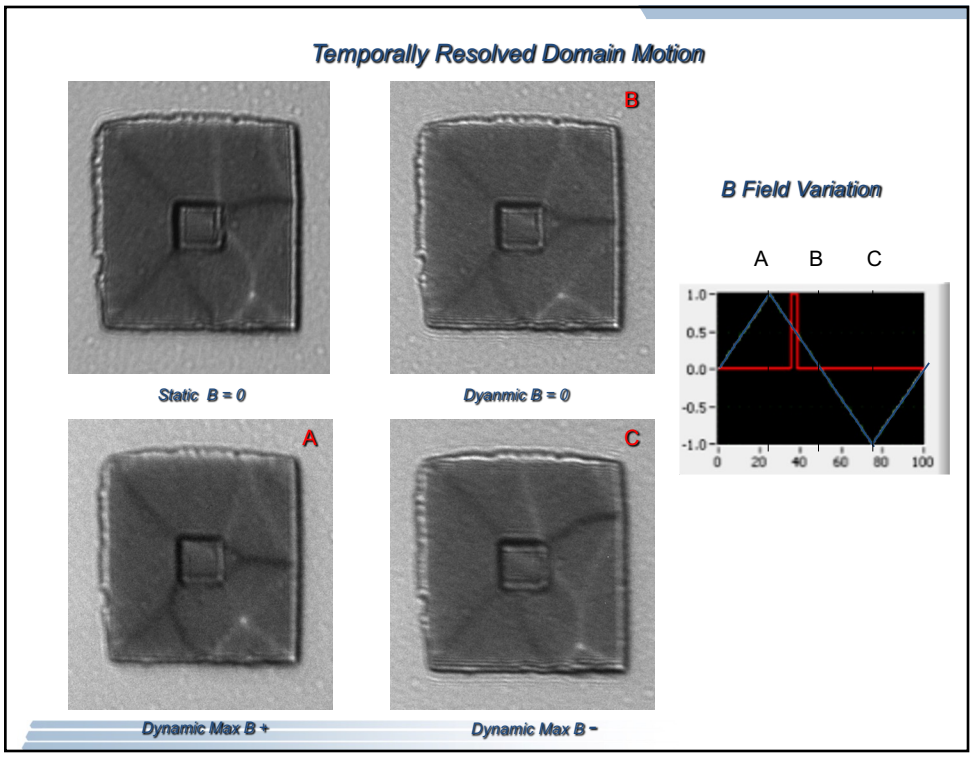
Temporally Resolved Domain Motion
B
Static B = 0
Dyanmic B = 0
B Field Variation
A B C
1.0
0.5
0.0
-0.5
-1.0
0 20 40 60 80 100
A
C
Dynamic Max B +
Dynamic Max B -

93

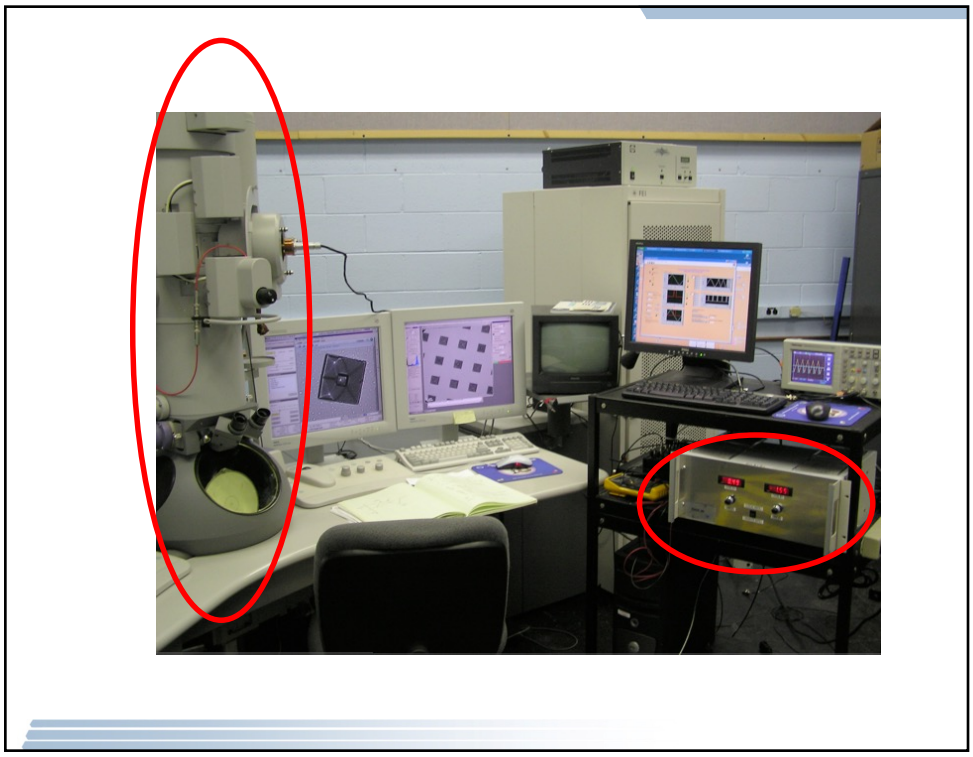

94

Lorentz Microscopy
TEM vs LSTEM

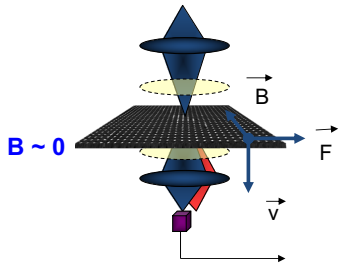

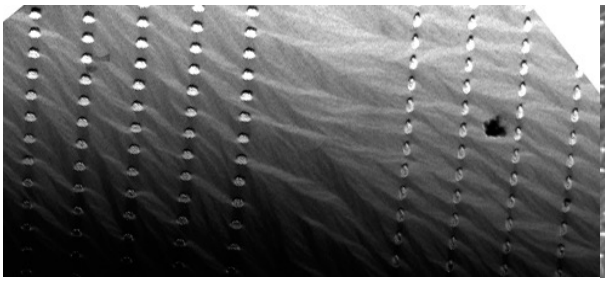

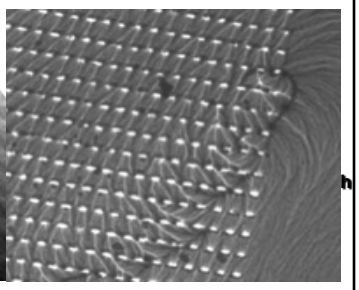

LSTEM TEM

95

Comparison STEM vs LSTEM

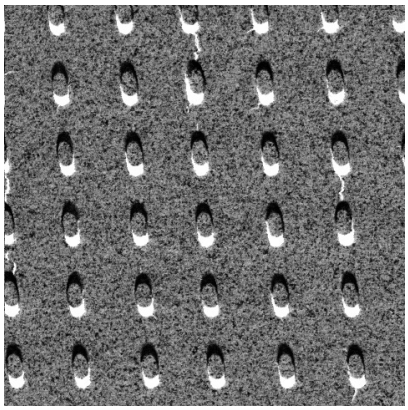

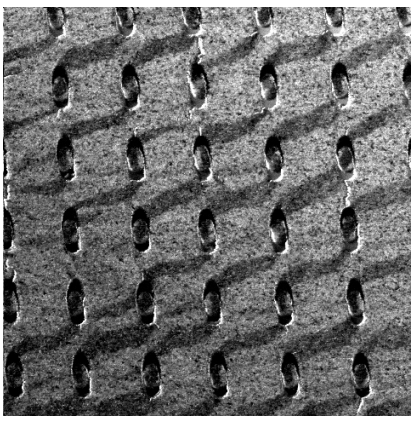

BF STEM LSTEM

96

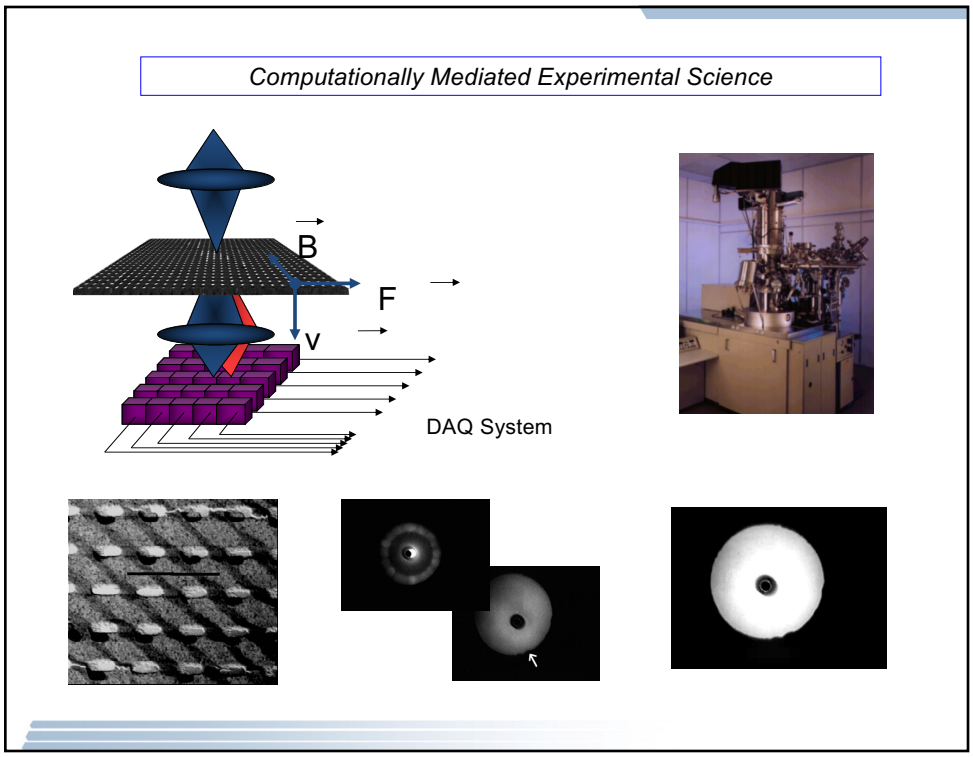
Computationally Mediated Experimental Science
B
F
v
DAQ System

97

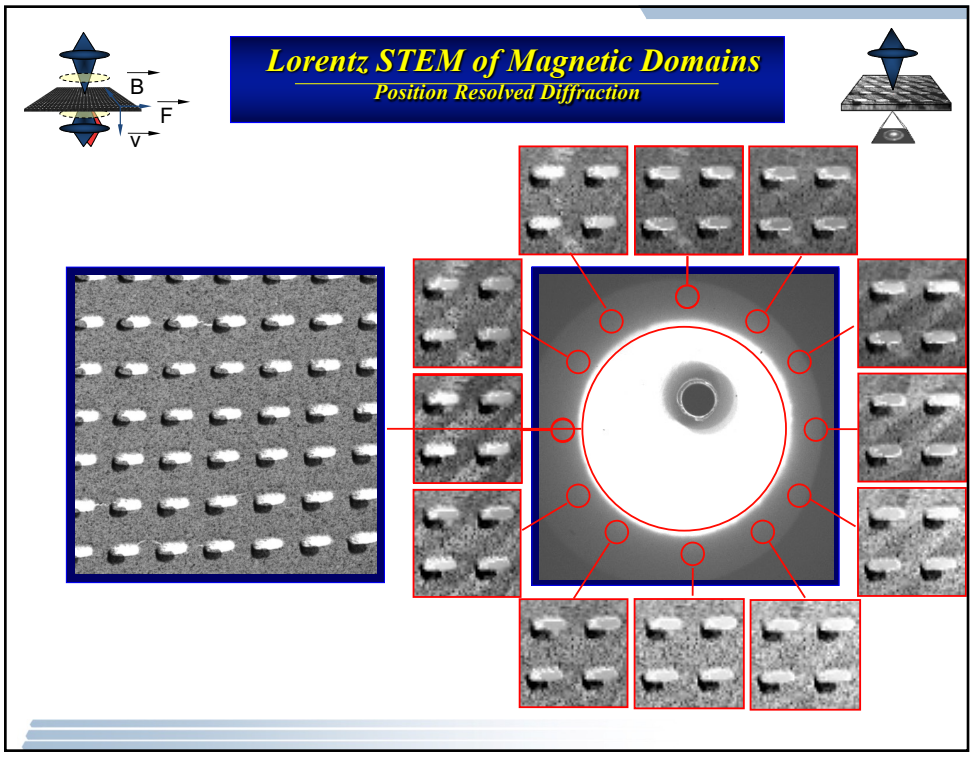
B
F
v
Lorentz STEM of Magnetic Domains
Position Resolved Diffraction

98

Electron Holography for High Spatial Resolution Magnetization Measurements

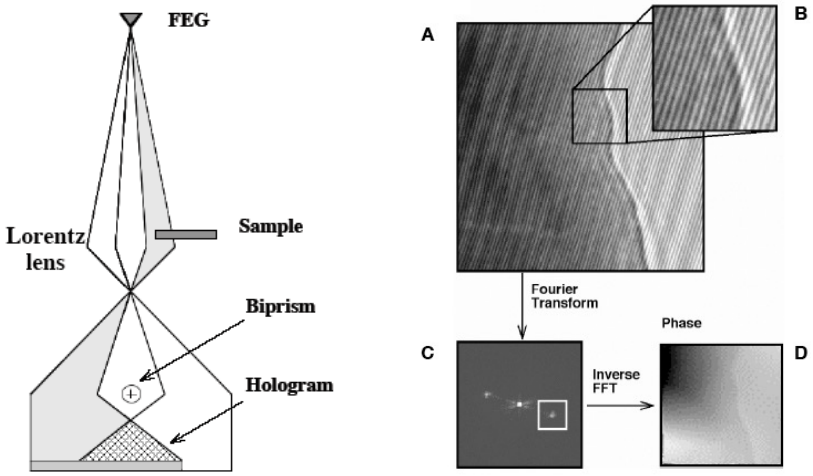

99

High Coherence Electron Holography

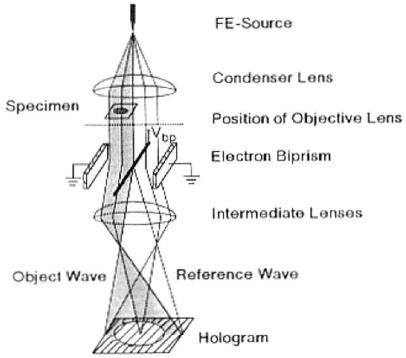

100

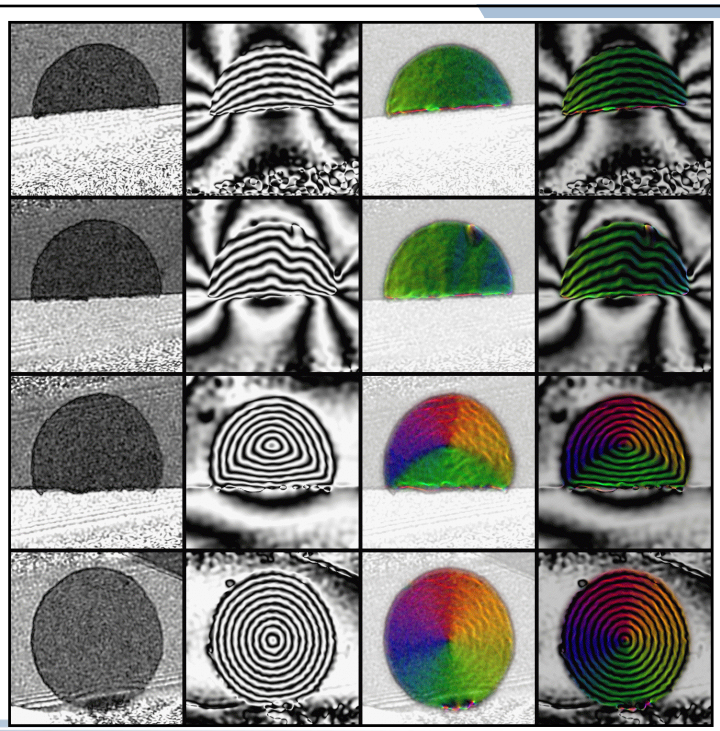

101

Ultra High Speed Imaging
Requirements: ~0.1 nm, <0.1 ns

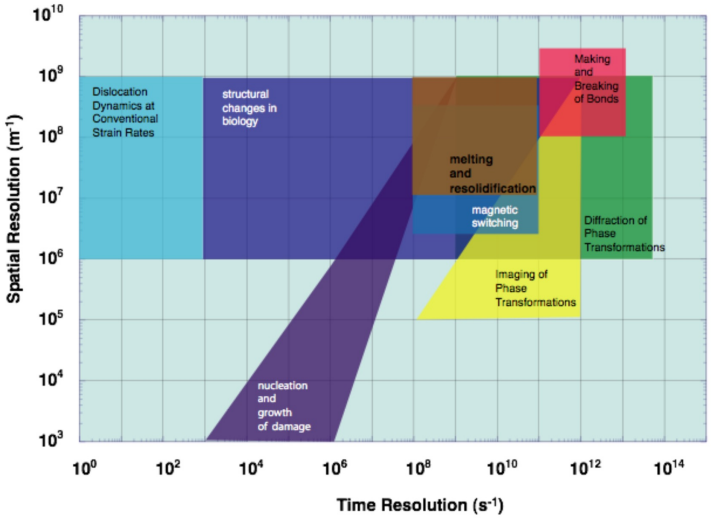

Courtesy of N. Browning UC Davis

102

Ultra High Speed Imaging
Requirements: ~0.1 nm, <0.1 ns

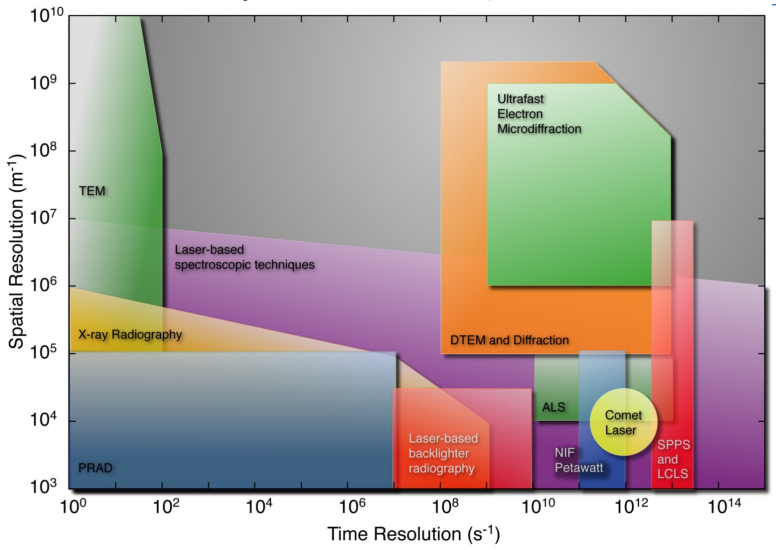

Courtesy of N. Browning UC Davis

103